



The classification and identification of human somatic and parasympathetic nerve fibres including urinary bladder afferents and efferents is preserved following spinal cord injury

G. Schalow

Abstract

Single-fibre extracellular action potentials were recorded with 2 pairs of wire electrodes from lower human sacral nerve roots during surgery. The roots from which was recorded from were used for morphometry. Nerve fibre groups were identified by conduction velocity distribution histograms of single afferent and efferent fibres and partly by nerve fibre diameter distribution histograms. The values of group conduction velocity and group nerve fibre diameter measured in the paraplegics were very similar to those obtained from brain-dead humans and patients with no spinal cord injury. Thus the classification and identification of nerve fibre groups remained preserved following spinal cord injury. Upon retrograde bladder filling the urinary bladder stretch and tension receptor afferent activities were increased; on two occasions they even fired when the bladder was empty. Two reasons are brought forward for a too small storage volume of the urinary bladder in paraplegics: too high afferent activity of the bladder due to changed receptor field transduction mechanisms and too low compliance.

Summary:

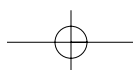
1. Single nerve fibre action potentials (APs) of lower sacral nerve roots were recorded extracellularly with 2 pairs of wire electrodes during an operation for implanting an anterior root stimulator for bladder control in 9 humans with a spinal cord injury and a dyssynergia of the urinary bladder. Roots that were not saved and that were used to record from were later used for morphometry.

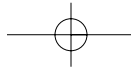
2. Nerve fibre groups were identified by conduction velocity distribution histograms of single afferent and efferent fibres and partly by nerve fibre diameter distribution histograms, and correlation analysis was performed. Group conduction velocity values were obtained additionally from compound action potentials (CAPs) evoked by electrical stimulation of nerve roots and the urinary bladder.

3. The group conduction velocities and group nerve fibre diameters had the following pair-values at 35.5°C: Spindle afferents: SP1 (65 m/s / 13.1 μ m), SP2 (51/12.1); touch afferents: T1 (47/11.1), T2 (39/10.1), T3 (27/9.1), T4 (19/8.1); urinary bladder afferents: S1 (41 m/s / -), ST (35/-); α -motoneurons: α_{13} (-/14.4), α_{11} (65 m/s / 13.1 μ m), α_{11} (60/12.1) [FF], α_2 (51/10.3) [FR], α_3 (41/8.2) [S]; γ -motoneurons: γ_β (27/7.1), γ_1 (21/6.6), γ_{21} (16/5.8), γ_{22} (14/5.1); preganglionic parasympathetic motoneurons: (10 m/s / 3.7 μ m).

4. The values of group conduction velocity and group nerve fibre diameter measured in the paraplegics were very similar to those obtained earlier from brain-dead humans and patients with no spinal cord injury. Also, the axon number and the axon density of myelinated fibres of lower sacral nerve roots remain unchanged following spinal cord injury. Thus the classification and identification of nerve fibre groups remained preserved following spinal cord injury. A direct comparison can thus be made of natural impulse patterns of afferent and efferent nerve fibres between paraplegics (pathologic) and brain-dead humans (supraspinal destroyed CNS, in many respects physiologic).

5. When changing the root temperature from 32°C to 35.5°C, the group conduction velocities changed in the following way in one case: SP2: 40 m/s (32°C) to 50 m/s (35.5%), S1: 31.3 to 40, ST: 25 to 33.8, M: 12.5 to 13.8; α_2 : 40 to 50, α_3 : 33 to 40. The group conduction velocities showed different temperature dependence apart from SP2 fibres and α_2 -motoneurons.





6. Upon retrograde bladder filling the urinary bladder stretch (SI) and tension receptor afferent (ST) activity levels were undulating and increased. As compared to activity levels detected in a brain-dead human, SI (designates afferents, not cord segment) and ST afferents fired even when the bladder was empty, with an activity level similar to those observed in a brain-dead human with the bladder half filled. Two reasons are brought forward for a too small storage volume of the urinary bladder in paraplegics: too high afferent activity of the bladder due to changed receptor field signal transduction mechanisms and too low compliance.

7. With the newly developed 'coordination dynamics therapy', applied early after spinal cord injury, such complications of bladder functioning can be avoided; the bladder can causally be cured in severe spinal cord injury.

Key-words: Human – Spinal cord injury – Urinary bladder – Dyssynergia – Single-fibre action potential – Conduction velocity – Nerve fibre diameter – Classification scheme – Bladder afferent activity – Electrical intravesical stimulation – Coordination dynamics therapy

Introduction

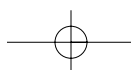
A movement and learning therapy, called coordination dynamics therapy, has been shown to be able to improve central nervous system (CNS) functioning after stroke (65), traumatic brain injury (66, 74), hypoxic brain injury (73), cerebellar injury (75, 76), spinal cord injury (67, 68, 84-87), in cerebral palsy (72), and in Parkinson's disease (69, 71).

The research in this and the following 4 articles in basic human neurophysiology and clinical research is aimed at developing cure for patients with spinal cord injury (35, 36, 41-44, 49) in general and to improve micturition, defecation and sexual function in particular. Recent review articles on the repair of the spinal cord injury concentrated on the regeneration of the spinal cord in animals, therapeutic potential of neural stem cells, and molecular mechanisms (79-82). These review articles did not include human research. The biggest problem among patients with spinal cord injury, namely how to cure urinary bladder functions, was also not reviewed. This current research project, on the other hand, approaches the problem, to cure spinal cord injury in human, differently. It concentrates on human research on the single neuron level, the integrative level of CNS organization, and the clinical level. It includes data from patients with spinal cord injury and brain-dead humans to compare the pathophysiologic with the physiologic CNS functioning to develop treatment. As will be shown, most of the dysfunctions of the urinary bladder can be understood by using the measured natural impulse pat-

terns of humans and functional anatomy. But to understand how to cure detrusor-sphincteric dyssynergia by changing the stability of the attractor states 'detrusor-sphincteric synergia' and 'dyssynergia', the 'System Theory of Pattern Formation (83) for Repair' (75, 86, 87), detailed anamneses of patients, and knowledge of movement learning, including learning transfer, has to be used. To improve the coordination between the activations of the somatic and parasympathetic nervous system divisions by stability changes, achieved by coordination dynamics therapy, integrative functions of the CNS have to be understood. Still, the essential step to cure partly spinal cord injury came from the measured natural impulse patterns in brain-dead humans by use of the single-nerve fibre action potential recording method, for which the author has been attacked ethically in the past. The goal of curing urinary bladder functions, following spinal cord injury, is achieved and will be presented in the last publication (78). No destructive operations are needed any more to improve urinary bladder functions. Bladder problems are not only faced by patients with spinal cord injury, but also by elderly people and young women after the birth of the first child (stress incontinence). 5% of the society suffers on incontinence.

Upon advancing with this basic human research, clinical consequences will be included and discussed in this and the following articles. The general clinical consequences will be discussed in the treatment paper (78).

This basic human research started from the scratch by first clarifying the necessary anatomy (35, 36,



41, 42) and developing a new basic human electrophysiological recording technique, the recording of single-nerve fibre extracellular action potentials (APs) with 2 pairs of wire electrodes from undissected nerve roots, a technique which can be used for intraoperative diagnosis and research (37, 39, 44).

The further development of the morphometry of nerves (classification of fibre diameters according to 4 myelin sheath thickness ranges) made it possible to simultaneously characterize nerve fibre groups by group conduction velocities and group nerve fibre

diameters (Fig. 1) (39, 45, 46). In this way, an exact classification scheme could be constructed for the human peripheral nervous system. The scheme is a solid basis for human neurophysiology and pathophysiology, even though it is incomplete and holds so far only for nerve fibre diameters larger than approximately $3.5 \mu\text{m}$. Another basic electrophysiological method for use on humans, the recording of single-nerve fibre extracellular APs with tungsten electrodes (57), made it possible to record impulse patterns of single nerve fibres; the method however

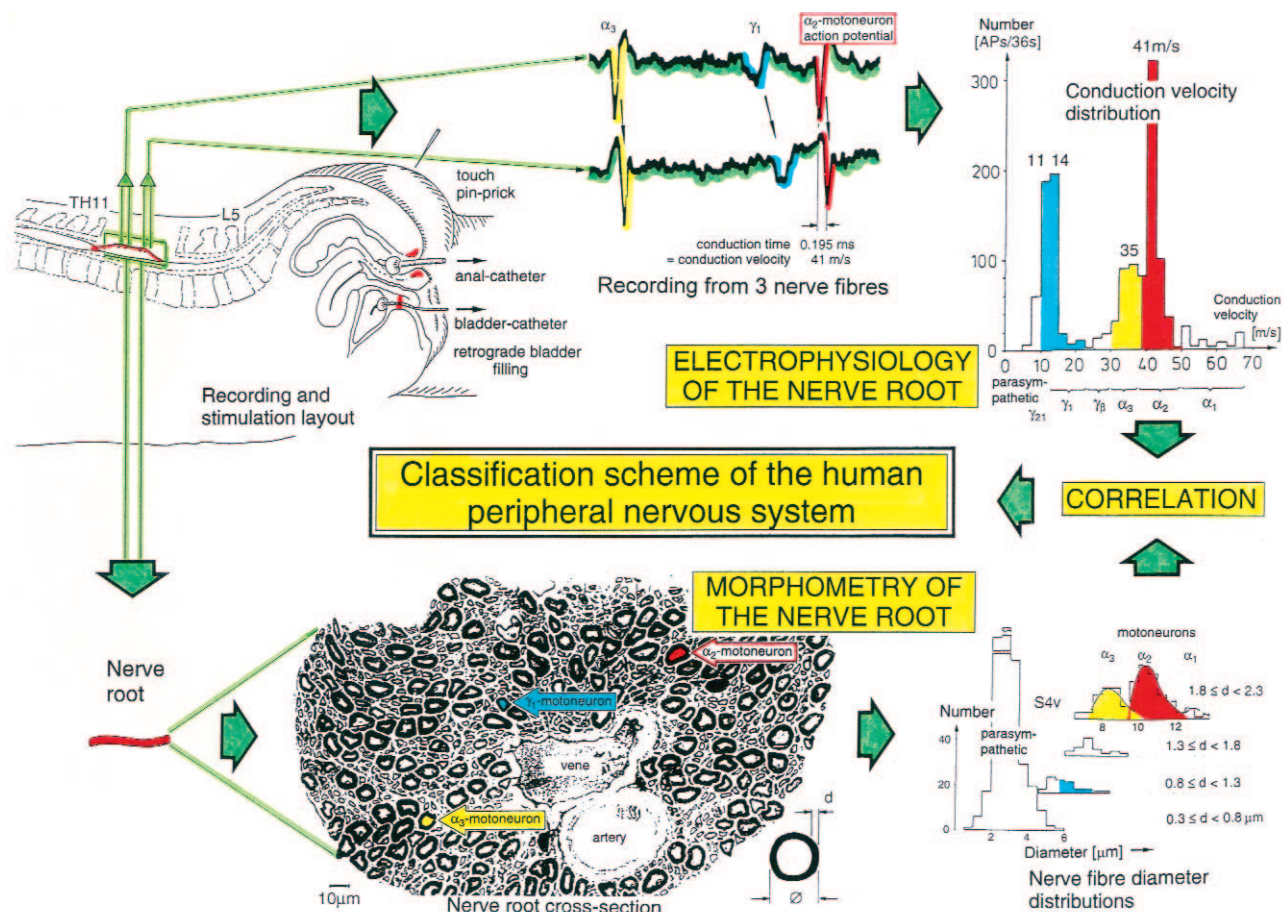


Fig. 1. – Schematic layout of the classification scheme for the human peripheral nervous system. By recording with two pairs of platinum wire electrodes from a nerve root containing approx. 500 myelinated nerve fibres, a recording is obtained in which 3 action potentials (APs) from 3 motoneurons (main AP phase downwards) can be seen. By measuring the conduction times and knowing the electrode pair distance (10 mm) a conduction velocity distribution histogram is constructed in which the nerve fibre groups are characterized by ranges of conduction velocity values and peaks in asymmetrical distributions. After recording, the root was removed, fixated, embedded and stained, light microscope cross-section were prepared and used to measure the mean diameter and the myelin sheath thickness (d). Distributions of nerve fibre diameters were constructed for 4 different ranges of myelin sheath thicknesses. Nerve fibre groups were characterized by the peak values of asymmetrical distributions. By correlating the peak values of the velocity distributions with those of the diameter distributions obtained from the same root, a classification scheme was constructed of human peripheral nervous system. Brain-dead human HT6.

rests on the peripheral nerve fibre classification schemes for animals which do not apply to humans.

The following up of time-dependent conduction velocity distributions of afferent and efferent fibres allows an analysis of activity level changes of nerve fibre groups. Urinary bladder afferent activity changes upon retrograde bladder filling (40) or motoneuron recruitment in nerve fibre groups are examples of this approach (47, 48). Since it is further possible to distinguish the APs from afferent and efferent nerve fibres and to extract from the summed activity of a fibre bunch the discharge patterns of single-fibres, it is possible to analyse receptor properties (44) and functions of the human central nervous system (CNS). An insight into the CNS functions can be obtained from simultaneous impulse patterns of single afferent and efferent fibres and from the phase relations between the impulses of afferents and efferents (49), following natural stimulation. With the discovery of the human spinal oscillators (40), CNS functions can be investigated based on the behavior of spinal oscillators for long lasting, rather constant, afferent input.

Since it is possible to record APs from preganglionic parasympathetic axons, to extract parasympathetic activity from secondary muscle spindle afferent fibre activity (49), and to partly correlate urodynamic parameters (bladder pressure) with the activity patterns of secondary muscle spindle afferent fibres (51), a simultaneous analysis of functions of the somatic and the parasympathetic nervous systems is possible. Such a simultaneous analysis allows the study of correlations between the somatic and the parasympathetic divisions occurring in micturition.

Materials and Methods

Measurements were collected from 9 (mean age of the patients = 27 years) humans with spinal cord lesions (Table 1 of 64), a dyssynergia of the urinary bladder, spastic pelvic floor, and spasticity in general. The electrophysiologic measurements were performed during surgery with the new method of recording single-fibre action potentials (APs) extracellularly from undamaged nerve roots or nerve root fascicles. The surgery was performed in order to implant a sacral anterior root stimulator (according to Brindley (7)) to improve bladder control and to

save the kidneys. This destructive operation is with the successful cure of urinary bladder functions (78) not justified any more. The strategy of the surgery is to deafferentiate the urinary bladder to increase its storage volume and to stimulate afterwards the motor roots (mainly S3 and S4) to empty the bladder. To deafferentiate the bladder, afferents and efferents in the nerve roots were identified by electrical stimulation and partly by using the single-fibre AP recording method to recognize afferents in certain roots. For the identification and the electrical stimulation after the operation, dorsal and ventral roots were separated or dissected if sticking strongly together. The extirpation of parts of dorsal roots is a part of the surgical procedure. Dorsal root fibres do further conduct 10 to 14 days following cutting. Their functioning is unsuitable for the electrical stimulation afterwards. Root parts were removed mostly between the spine segments L4 and S2; that is about the middle part of the S5 root and a more caudal part for the S2 root. Slight damage may have occurred with the handling of the roots and slight desiccation may have occurred, when removing the roots. The not removed ventral roots were functioning well after the operation. Cut dorsal roots, from which recording was performed, were fixated and prepared for morphometry (Fig. 1). One ventral S4 root was obtained because of an accidental cut (happens seldom). Light anesthesia (paraplegics feel no pain) was administered with Propofol, not to reduce the AP amplitude too much. Intraoperative recording times were less than 0.5 hours. The heart rate during the operation was around 55/min (para 4, 85), the blood pressure was in the range 95/60 (para 5, 130/85). When with the electrical stimulation of the dorsal roots (for clarifying the representation of bladder afferents and efferents in the sacral roots) the systolic blood pressure increased over 140, it was waited for further electrical stimulation till the blood pressure decreased. The respiratory rate was between 10 and 13/min, the O₂ saturation was mainly between 97 and 100%, and the CO₂ expir. was mainly between 4.0 and 4.5%.

Electrophysiology

Single-fibre APs were recorded extracellularly (Fig. 1) from nerve roots with 2 platinum wire elec-

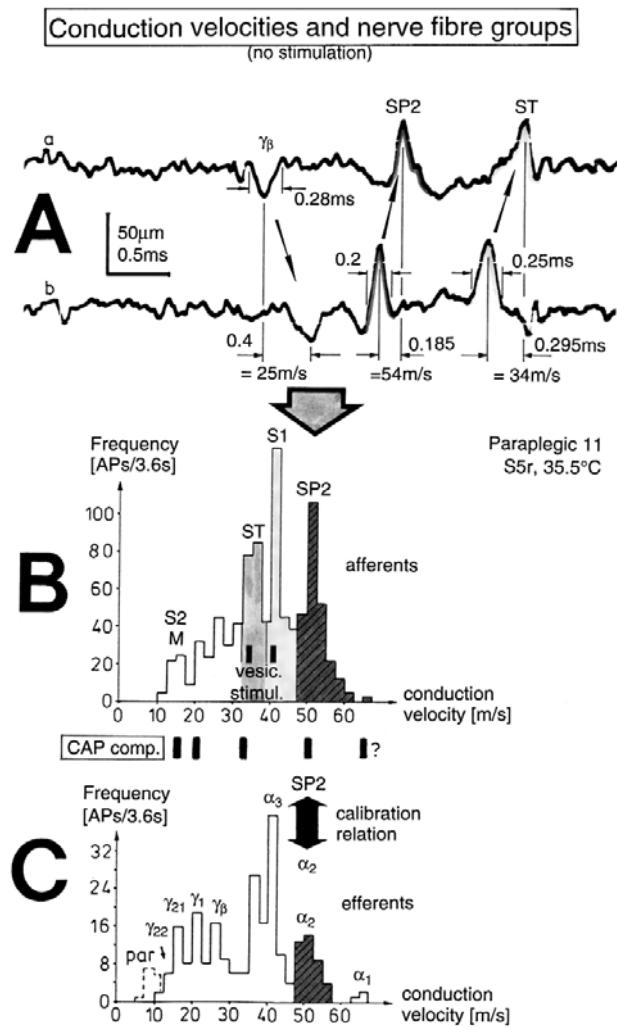


Fig. 2. – A. Sweep piece of recording; conduction times and corresponding conduction velocities are indicated. Root temperature at recording, 35.5°C.

B, C. Conduction velocity distributions of afferents (B) and efferents (C) obtained for a time interval of 3.6 s with no additional stimulation. SP2 = secondary muscle spindle afferents, S1 = stretch receptor afferents of bladder, ST = tension receptor afferents, M = mucosal afferents, S2 = afferents responding to fluid movement; α_1 = α_1 -motoneurons (FF), α_2 = α_2 -motoneurons (FR), α_3 = α_3 -motoneurons (S), γ_B = γ_B -motoneurons, γ_1 = γ_1 -fusimotors (dynamic), γ_{21} = γ_{21} -fusimotors (static), γ_{22} = γ_{22} -fusimotors (static), par = preganglionic parasympathetic motoneurons. CAP comp. = group conduction velocities obtained from the components of compound action potentials (CAPs). Vesic. stimul. = group conduction velocities of bladder afferents obtained upon electrical intravesical stimulation (see Figs. 8, 9). Calibration relation indicates the same peak group conduction velocity of secondary spindle afferents and α_2 -motoneurons (cross-hatched). Velocity histogram classes \leq and $<$ (half closed (left) interval).

trode pairs (electrode pair distance = 10 mm; electrode distance in each pair = 4 mm) at 2 sites, preamplified ($\times 1000$), filtered (RC-filter, passing frequency range 100 Hz-10kHz) and displayed on a digital storage oscilloscope (Vuko Vks 22-16), and also stored using a PCM-processor (Digital Audio Processor PCM-501ES) and a video recorder. The beginning of a touch or a pin-pricking was marked with an upward pulse; and the end with a downward pulse on trace „a“. These pulses were generated by a markation pulse generator connected to the digital scope, which was switched on and off with a touch sensor working on the basis of resistance changes. Also the pulling and releasing of anal and bladder catheters were mostly marked with the help of pull-switch connected to the catheters and working in connection with the same markation pulse generator. Trace „a“ was the recording from the proximal electrode pair and trace „b“ from the distal pair. Conduction velocities of single-fibres were calculated from the conduction distance (electrode pair distance) and the respective conduction times, the time needed for an AP to cover the conduction distance (time difference between traces „a“ and „b“ for a particular AP). APs from afferents and efferents could clearly be distinguished since for the used electrode arrangements the main phase (second phase) from afferent fibres is upwards and that of efferents downwards (Fig. 2A). E.g., the AP of a skin afferent fibre reaches a pair of electrodes first as negative and then as positive. According to the electrode setting used, the main phase is upwards. An AP of a motoneuron, coming from the opposite direction, would reach the electrodes in the order positive-negative. The potential changes are therefore opposite and the main triphasic AP will point downwards. An AP in an afferent fibre reaches first the caudal electrode pair and then the rostral pair, whereas an AP of the efferent fibre reaches first the rostral electrode pair and then the caudal one. The conduction times are therefore also opposite (Fig. 2A). If APs of two efferent fibres meet at one electrode pair at the same moment, the APs add up algebraically. The adding up of many fibres' impulses, following electrical stimulation will give rise to a compound AP (50). If the APs of an afferent and an efferent fibre meet at the same point of time at one electrode pair, they partly or fully abolish each other (subtraction of the AP

amplitudes). However since these APs will not meet each other at the other electrode pair, the afferent and the efferent APs are clearly distinguishable on the trace of the other electrode pair. The conduction velocities of afferent APs were plotted in an afferent conduction velocity distribution histogram (Fig. 2B) and those from efferent APs in an efferent velocity histogram (Fig. 2C). Histogram classes were half closed intervals (\leq and $<$); the left border belongs to a particular class, the right one does not. Group conduction velocity and nerve fibre diameter values were the peak values of asymmetrical distributions. Single-fibre APs were always recorded from whole roots or fascicles. I did not try to tease single-fibres. In nerve roots thinner than 0.6 mm in diameter (radial decline of AP amplitude due to volume conductance is approx. by a factor of 1/10 per 0.3 mm; the root flattens when positioned on the wire electrodes), it is possible to record single-fibre APs from all fibres with a diameter larger than approx. 4 μm . The radial decline of low-amplitude long-lasting extracellular APs, due to volume conductor embedding, of thin fibres, including preganglionic parasympathetic fibres, is less pronounced than it is for high-amplitude short-lasting APs since the low frequency sinusoidal coefficients will have large amplitudes in a Fourier-expansion (17, 32). Since nerve roots have no epineurium and nearly no perineurium, the nerve fibres in the roots can easily be damaged when recording with wire electrodes. Pressure and stretch will change the AP wave form or even block conduction (most easily at the node of Ranvier) so that an AP can be recorded from one electrode pair only. Double peaked APs can occur, probably when a node of Ranvier is blocked. Mechanical stimulation, nerve fibre compression, resistance artifacts and trigger zones may change impulse shape and activity (23, 26, 33, 34, 55, 58, 60, 61). For further literature see Ref. (38). Heavily distorted APs from damaged fibres were omitted from the analysis.

Morphometry

Pieces a few cm long were removed from dorsal roots which were used to record from, fixated for 4 hours in 4% glutaraldehyde in cacodylate buffer, afterfixated in 1% OsO_4 for 2 hours, and dehydrated

and embedded in Araldite according to standard techniques. Pictures of semi-thin sections (approximate depth = 1 μm) stained with thionin acridine-orange, were taken with a light microscope ($\times 1000$). Nerve fibre diameters $\bar{\varnothing} = 1/2(\varnothing_1 + \varnothing_2)$ (\varnothing_1 and \varnothing_2 are the larger and the smaller diameter of non-round shaped fibres) and the mean myelin sheath thickness „d“ were measured by hand. A shrinkage correction of 8% was allowed. The nerve fibre diameters measured were divided into 4 ranges of myelin sheath thickness: $0.25 \mu\text{m} \leq d < 0.8$; $0.8 \leq d < 1.3$; $1.3 \leq d < 1.8$; $1.8 \leq d < 2.5 \mu\text{m}$. For each class of myelin sheath thickness a diameter distribution histogram was constructed. In the case of damaged fibres (splitted myelin sheath) the myelin sheath thickness was measured at the most preserved part. Very strongly damaged fibres were not taken into consideration. Because of the preference of the authors of even to odd values, neighbouring histogram classes show large variations. This systematic error can be abolished by increasing the width of the histogram classes from 0.25 μm to 0.5 μm . For the diameter distribution $0.25 \leq d < 0.8 \mu\text{m}$ the higher histogram class was used anyway. Computer-assisted morphometry would eliminate such systematic error, but would have less accuracy, since computer programs cannot handle artefacts and altered nerve fibres as if they were normal fibre. Electron micrographs were only used to check the light microscope pictures.

Ethics

Informed consent was obtained from the patients to the recordings to be made. The method of recording single-fibre APs was used for intraoperative diagnosis, to identify more safely (e.g. in the case of an anatomical variation) what nerve fibres are contained in what nerve root fascicles. An improvement of the intraoperative diagnosis may make it possible in the future to deafferentiate the bladder more specifically. It would be of great benefit if one could save e.g. the afferents signalling sexual sensation. This qualified but destructive operation is not justified any more, because urinary bladder function can be repaired by functional reorganization and regeneration of the human spinal cord (78, 86, 87).

Results

Conduction velocity distributions for afferent and efferent nerve fibres

From 9 paraplegics (para 3 to para 11) with spinal cord lesions for 0.5 to 6 years single nerve fibre action potentials (APs) were recorded extracellularly from sacral nerve roots during the surgery, conduction velocities were calculated and group conduction velocities were determined from the peaks in the velocity distribution histograms. The measured peak values of the group conduction velocities for all paraplegics are summarized in Table 1 of 64. The patients, aged 20 – 37 years, suffered from dyssynergia of the urinary bladder, had a spastic pelvic floor and showed spasticity of different degree in general. They underwent surgery for the implantation of a sacral anterior root stimulator (destructive opera-

tion) to enable urinary bladder control (Table 1 of 64). Upon electrical stimulation of the ventral roots (often S3 plus S4), the external bladder sphincter and the detrusor contract. Since the external bladder sphincter (striated muscle) relaxes earlier than the detrusor (smooth muscle) following the impulse train, urine emerges from the bladder. Repeated stimulation empties the bladder.

From single nerve fibre AP recordings, like those in Figs. 2A and 3D, conduction velocity frequency distribution histograms were constructed for single-fibres with no additional stimulation (Fig. 2B, C) and measurements obtained during changing of a thin for a thick anal catheter (Fig. 3E, F). Following anal catheter stimulation the peak of preganglionic parasympathetic fibres appeared (Fig. 3F), indicating that the parasympathetic division was activated. The activation of the parasympathetic division will be tackled in a following paper (51). The identification of nerve fibre groups from conduction velocity distributions rests upon the assumption that nerve fibres of a certain group conduct at a velocity similar to those obtained from measurements in brain-dead humans (HTs) and in patients with no spinal cord lesion (39). Further support for the use of these single-fibre conduction velocity distributions with group identification was obtained from electrical nerve root stimulation (50) and electrical intravesical stimulation (Figs. 9, 10).

Electrical nerve root stimulation with the Brindley stimulator (7) evoked compound action potentials (CAPs) the components of which were conducted at velocities similar to the group conduction velocities obtained from single-fibre AP recordings showing natural impulse patterns. Because of a large number of afferent and efferent nerve fibre groups contained in the roots only few CAP components were obtained. The fast conducting groups of secondary muscle spindle afferents (SP2), conducting orthodromically, and the α_2 -motoneurons (FR), conducting antidromically if stimulated caudal to the recording electrodes (or vice versa if stimulated rostrally), could nevertheless be extracted from the CAP components. Because of time restrictions during the surgery, electrical stimulation at the thresholds of the different groups was only performed occasionally so that the CAPs often did not split into different components. Also, due to insufficient space the stimulation electrodes were positioned approx. 2 cm ros-

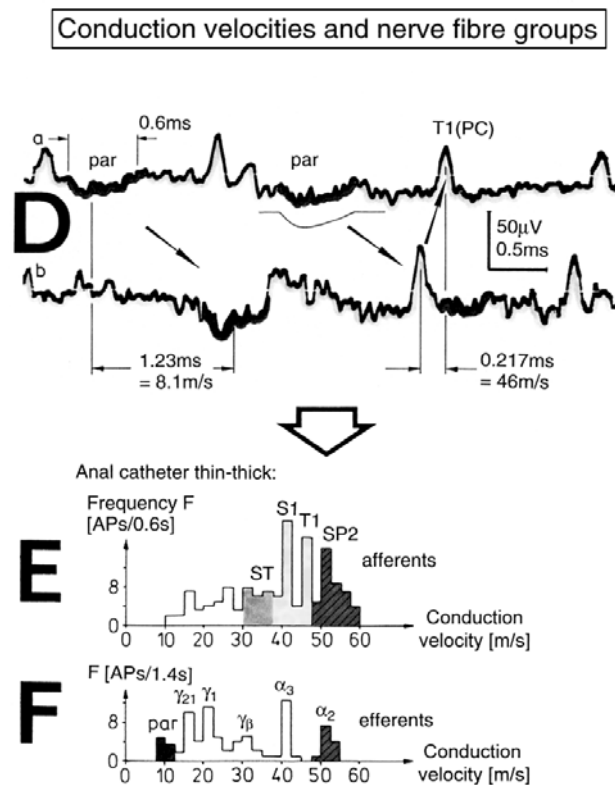


Fig. 3. – Sweep piece of recording (D) and conduction velocity distributions (E,F) taken from time intervals following a change of a thin anal catheter ($\varnothing = 12$ mm) for a thick one ($\varnothing = 20$ mm). Note the manifestation of the parasympathetic peak. For symbols, see legend Fig. 2.

tral or caudal to the recording electrodes; for strong stimulations this resulted in a partial fusion of the stimulation artifact and the CAP. Anyhow, the group conduction velocity values obtained from the components of the CAPs have confirmed the group conduction velocity values obtained from single afferent and efferent nerve fibres (Table 1 of 64).

CAPs evoked by electrical intravesical stimulation (Fig. 9A), also performed with the Brindley stimulator (pulse duration 0.3 ms), were conducted at group conduction velocities very similar to those obtained for single stretch (S1) and tension receptor afferents (ST) of the urinary bladder (Fig. 2B).

Fibre diameter distributions for afferent and efferent nerve fibres

After the recording of single-fibre APs, the dorsal nerve roots were removed, fixated and prepared for morphometry. Figs. 4A,B,6B show examples of nerve root cross-sections obtained. Manually determined values of mean nerve fibre diameters ($1/2(\varnothing_1 + \varnothing_2)$) and mean myelin sheath thicknesses d (and of other parameters) were used to construct nerve fibre diameter distribution histograms (Figs. 5A, B, 6C). Nerve fibre groups were identified with the help of conduction velocity distribution histograms and the assumption that nerve fibre group diameters had not changed too much from physiologic values. The identification was started with the thickest fibres. Identified peaks were assigned to the group to which they belonged (see Fig. 5).

The presence in the lower sacral nerve roots of ventral root afferents and dorsal root efferents complicated the group identification from nerve fibre diameter peaks. This problem did not arise with conduction velocity distributions since APs from afferents and efferents have opposite triphasic amplitude and opposite conduction times. Also, velocity distribution peaks could partly be identified by different kinds of stimulation. With electrical intravesical stimulation for example, bladder afferents will mainly be activated whereas stimulation of the parasympathetic division will activate parasympathetic motoneurons.

As can be seen from Figs. 5A, B, 6C, the muscle spindle afferents, the 4 thickest skin afferents and the α -motoneurons had myelin sheath thicknesses

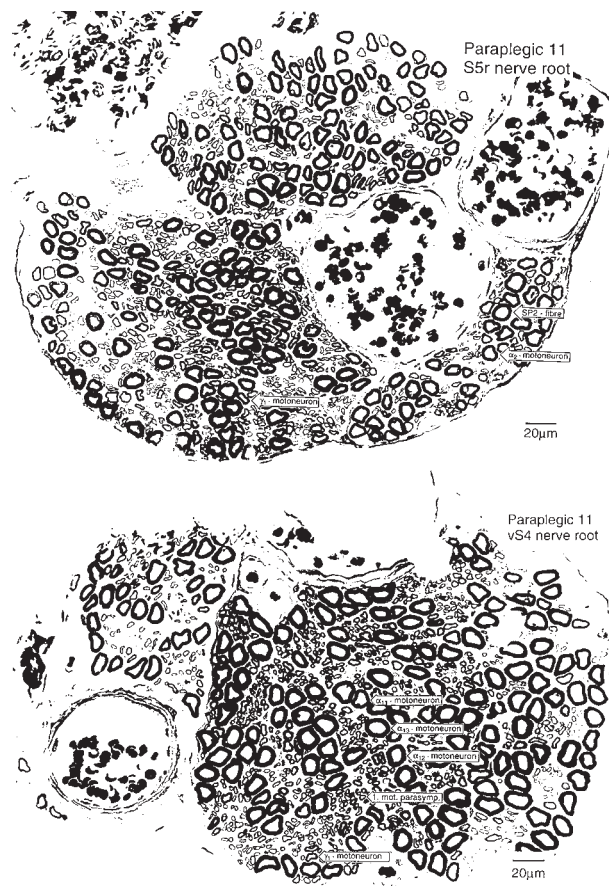


Fig. 4. – A. Light microscopic picture of a cross-section of the right nerve root S5. Nerve fibres are indicated which, according to their mean fibre diameter and myelin sheath thickness, most likely are a secondary muscle spindle afferent fibre (SP2), a γ_1 or an α_2 -motoneuron.

B. Light microscopic picture of a cross-section of a vS4 nerve root. Nerve fibres are indicated which, according to their mean diameter and myelin sheath thickness, are a preganglionic parasympathetic motoneuron, γ_1 , α_{11} , α_{12} , or α_{13} -motoneuron. Thionin acridine-orange staining of the myelin sheath. Paraplegic 11.

between 1.8 μm and 2.5 μm . The fusimotor fibres ($\gamma_1 - \gamma_{22}$) had myelin sheath thicknesses between 0.8 μm and 1.3 μm , and the preganglionic parasympathetic motoneurons between 0.25 and 0.8 μm . Only few axons had myelin sheaths with a thickness between 1.3 μm and 1.5 μm . In dorsal roots there were only few fibres with a myelin sheath thickness between 0.8 and 1.3 μm . The classification of nerve fibre diameters into 4 different ranges of myelin sheath thickness has the advantage that certain nerve fibre groups fit mainly within certain myelin sheath thickness ranges and can therefore

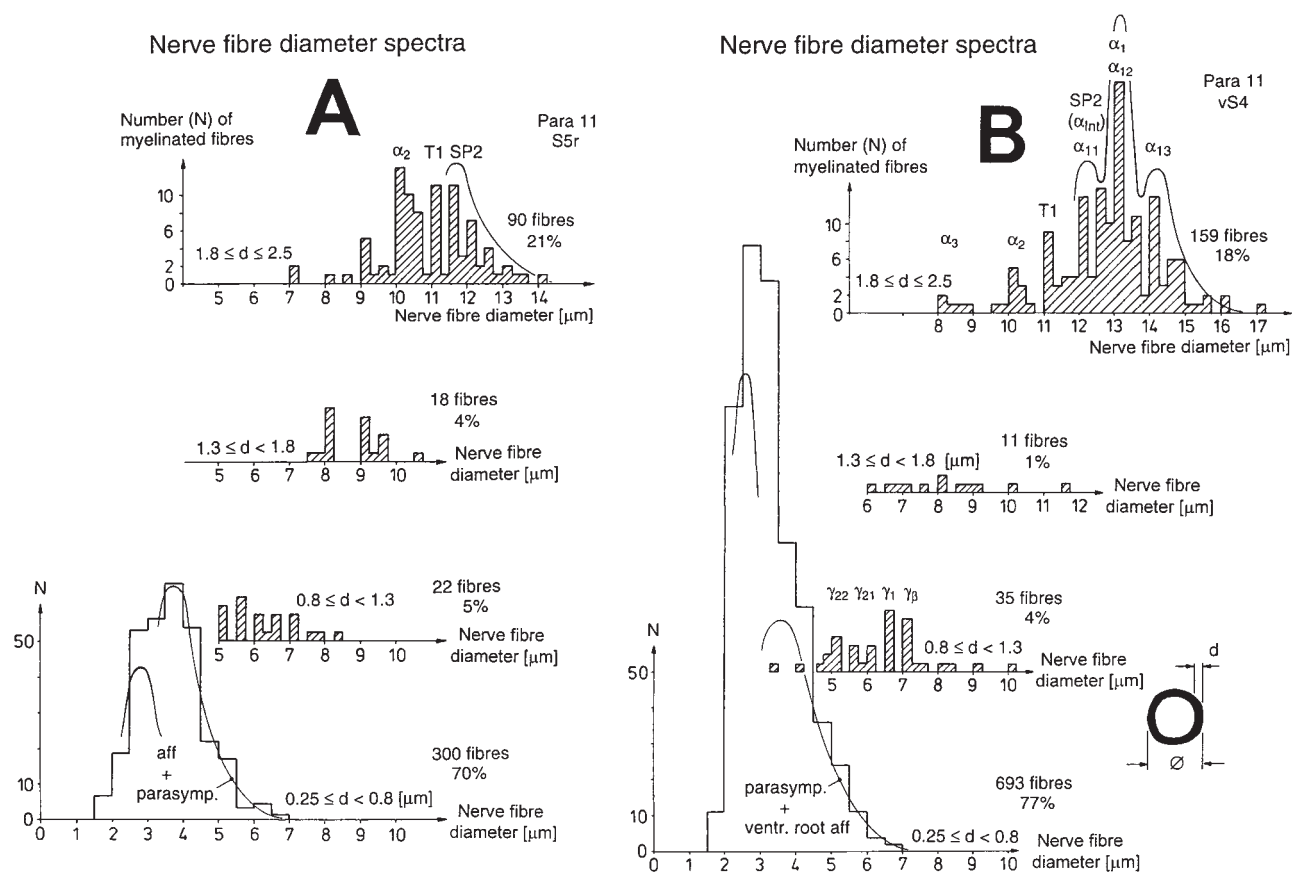


Fig. 5. – A. Nerve fibre diameter distributions of the right nerve root S5 (from Fig. 4A); classification in 4 ranges of myelin sheath thicknesses (d). Fibre diameter peaks are indicated, which represent α_2 -motoneurons, T1 skin afferents (PC), secondary spindle (SP2) afferents (aff) and preganglionic parasymphetic (parasymp.) nerve fibres. A distribution curve for SP2 fibres is indicated. In the range of myelin sheath thicknesses $0.25 \leq d < 0.8 \mu\text{m}$, possible fibre distributions are drawn into the histogram, which represent parasymphetic fibres and afferent fibres. B. Nerve fibre diameter spectra for nerve root vS4 (from Fig. 4B), according to 4 classes of myelin sheath thicknesses (d). Fibre diameter peaks are indicated, which represent γ_{22} , γ_{21} , γ_1 , γ_β , α_3 , α_2 , α_{11} , α_{12} , and α_{13} -motoneurons, parasymph. = preganglionic parasymphetic fibres, ventr. root aff = ventral root afferents. Paraplegic 11. The high number of α_1 -motoneurons (FF) in root S4 is unusual. Distributions of subgroups α_{11} , α_{12} and α_{13} are qualitatively drawn for α_1 -motoneurons. In the class of myelin sheath thicknesses $0.25 \leq d < 0.8 \mu\text{m}$, distribution curves are qualitatively drawn for parasymphetic fibres (parasymph.) and ventral root afferents.

be better identified. E.g., the parasymphetic preganglionic motoneurons have similar diameters as do the static fusimotors (γ_{22}) (Fig. 5B). They can be distinguished from each other by a thicker myelin sheath of the γ_{22} -motoneurons.

In human there are approximately 20% ventral root afferents and dorsal root efferents in the S4 root, 1-2% in the S3 root and less than 1% in the S2 root (46). Because of the myelinated ventral root afferents in the ventral S4 root, the fibres in the myelin sheath thickness class $0.25 \leq d < 0.8 \mu\text{m}$ (Fig. 5B) represent not only parasymphetic motoneurons

but also afferent fibres, whereas the fibres in the dorsal S2 root represent mainly afferents (Fig. 6B) in the myelin sheath thickness range $0.25 \leq d < 0.8 \mu\text{m}$. By plotting the distributions of thin myelin sheath fibres with reduced amplitude (Fig. 5B) into Fig. 6C (dashed line) one can compare the mixed parasymphetic-afferent fibre distribution with that of pure afferent fibre distribution. It can be estimated that parasymphetic preganglionic fibres (peak group diameter approx. $3.5 \mu\text{m}$) have a group diameter by approx. $0.6 \mu\text{m}$ thicker than the thin afferent fibres in the same myelin sheath thickness range, even

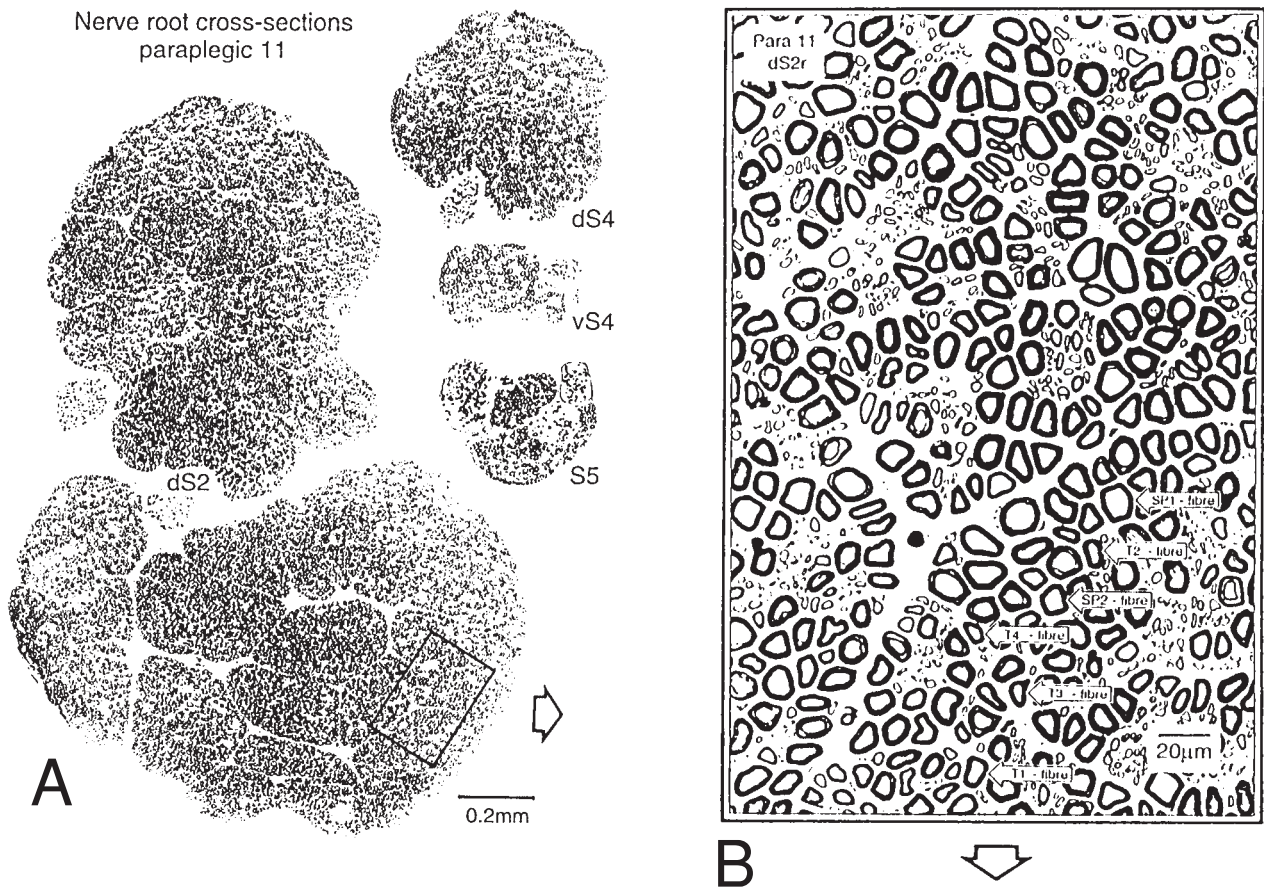
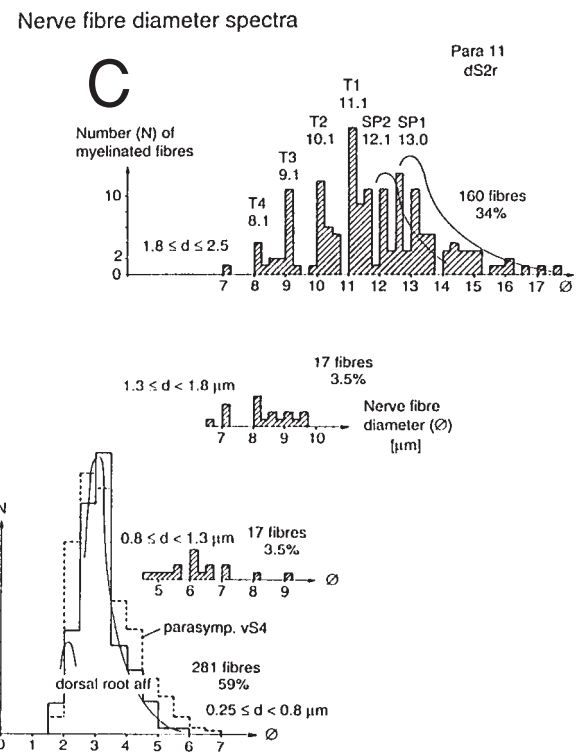


Fig. 6. – A. Cross-sections of the right nerve roots S5, vS4, dS4, dS2. The dorsal root S2 consists of 2 main fascicles. The square area marked in the lower fascicle of the S2 cross-section is shown in B at a higher magnification.

B. Magnified area of the dS2 cross-section from A. Nerve fibres are marked which, according to their diameter and myelin sheath thickness most likely represent primary spindle (SP1), secondary spindle afferent fibres (SP2) and T1 (PC), T2, T3, and T4 skin afferent fibres.

C. Nerve fibre diameter spectra of the dS2 cross-sectional area in B according to 4 ranges of myelin sheath thicknesses (d). Fibre diameter peaks are indicated, which represent primary (SP1) and secondary muscle spindle afferents (SP2), and the myelinated skin afferent fibres T1 (Pacianian corpuscle), T2, T3 (probably SAI) and T4. Distribution curves for SP1 and SP2 fibres are indicated. The histogram for parasympathetic fibres (including ventral root afferents) from root vS4 in Fig. 5B is represented by the dashed line (parasymph. vS4). The histogram for thin fibres ($0.25 \leq d < 0.8 \mu\text{m}$) includes possible afferent fibre distribution curves. Paraplegic 11. For further abbreviations and symbols see legend to Fig. 11.



though the distributions may not be identical. This numerical characteristic was already recognized during manual measurements of fibre diameters and myelin sheath thicknesses. Only seldom fibres were found in the dS2 root (Fig. 6B), with medium diameters and very thin myelin sheaths. The qualitatively drawn distribution curves of parasympathetic pre-ganglionic motoneurons and afferent fibres in the myelin sheath thickness class $0.25 \leq d < 0.8 \mu\text{m}$ (Figs. 5A, B, 6C) slightly help to differentiate between afferents and parasympathetic efferents; as indicated in Fig. 6C however, the afferent fibre distribution itself most likely includes more than a single-fibre group with the different groups having similar peak group diameter values.

The fibre diameter distribution of the secondary muscle spindle afferents (SP2) in the myelin sheath thickness range $1.8 \leq d < 2.5 \mu\text{m}$ (Fig. 5A) was qualitatively constructed by broadening the histogram classes and subsequent drawing the distribution curve. The SP2-fibre distribution was then drawn into the thick fibre distribution of the right dS2 root for the same patient (Fig. 6C). Now it is possible to draw qualitatively the distribution of the primary spindle afferents (SP1) again after broadening the histogram classes. The urinary bladder stretch (S1) and tension receptor afferents (ST) have group conduction velocities between those of touch 1 (T1) and touch 2 (T2), and between T2 and touch 3 (T3) skin afferents (Table 1 of 64) (for nomenclature see also Fig. 11). The group diameters of the bladder afferents may therefore be within the $9 \mu\text{m} - 11 \mu\text{m}$ range. But as Table 1 of Ref. 64 shows, the conduction velocities and the fibre diameters are not simply linked by a unique scaling factor in the range of 6. For the determination of more exact values, see the Discussion section.

The fibre class of α_1 -motoneurons represented in Fig. 5B seems to split up into 3 subgroups (α_{11} ($= \alpha_{int}$), α_{12} , α_{13}) in similarity to the results of measurements in dogs (45). The subpeaks have been drawn qualitatively. Again ventral root afferents (T1, SP2) disturb the motor fibre distribution. As expected, the different γ -motoneuron classes can be found in the myelin sheath thickness class $0.8 \leq d < 1.3 \mu\text{m}$.

Fig. 6A shows a comparison of the sizes of different roots measured in paraplegic 11. It can be seen that the root dS4 has approximately twice the

thickness of root S5 and twice the thickness of root vS4. Root dS2 is approximately 4 times as thick as root dS4.

In Figs. 4A, B, 6B, some afferent and efferent fibres are marked with the groups to which they belong. This assignment rests purely on the nerve fibre diameters and the myelin sheath thicknesses. As can be seen from the diameter distribution histograms, there also is reasonable probability that these fibres belong to adjacent fibre classes, because of overlaps of adjacent group distributions; also, fibres of so far not identified fibre groups could be represented by those fibres. Anyhow, these fibre designations clearly show that it is detailed morphometry only that can partly reveal the distinct nerve fibre groups.

Correlation between group conduction velocities and group nerve fibre diameters

All the measured peak values of group conduction velocities and group nerve fibre diameters are summarized in Table 1 of Ref. 64. The nerve roots used for electrophysiologic and morphometric determinations yielded a direct correlation between group conduction velocities and group nerve fibre diameters. As can be seen from Table 1, the group diameters vary only little from patient to patient, whereas the group conduction velocities vary quite much. The large variations of group conduction velocities are mainly due to different root temperatures, which are effected by the central temperature of a patient (34.3°C to 35.8°C). The temperature dependence of the conduction velocity is tackled below.

The following velocity-diameter pairs of afferents and efferents were obtained from Table 1 of 64 at $\sim 35.5^\circ\text{C}$:

α_{13} (-/14.1), α_{12} (65 m/s /13.1 μm), α_{11} (60?/12.1), α_2 (51/10.3), α_3 (41/8.2), γ_β (27/7.1), γ_1 (21/6.6), γ_{21} (16/5.8), γ_{22} (14/5.1), par(10/3.7).

SP1(65/13.1), SP2(51 m/s /12.1 μm), T1(47/11.1), T2(39/10.1), T3(27/9.1), T4(19/8.1), S1(41/-), ST(35/-).

As will be discussed below, the group conduction velocities and the group nerve fibre diameters of paraplegics are very similar to those obtained from brain-dead humans (Table 1 of Ref. 39) and patients with no spinal cord lesion (Fig. 11).

Temperature dependence of group conduction velocities

In all measured cases, the AP durations decreased and the conduction velocities increased of the single nerve fibres with increasing temperature. It seemed further as if the different nerve fibre groups had different temperature dependences, because for lower temperatures it was much more difficult to identify the different nerve fibre groups by their peaks in the velocity distributions. The operational field was therefore often warmed with an infra-red lamp to bring the root temperature as close as possible to 36°C.

In paraplegic 11, good conduction velocity distribution histograms from the same root under the same recording conditions were obtained for low (32°C) and for high (35.5°C) root temperatures. The secondary muscle spindle afferents (SP2) and the α_2 -motoneurons increased their conduction velocity from 40 to 50 m/s (25% increase), the S1, ST and M afferents from 31.3 to 40 (28%), from 25 to 33.8 (35%) and from 12.5 to 13.8 m/s (10%) respectively with increasing temperature. The α_3 -motoneurons increased their conduction velocity from 33 to 40 m/s (21% increase). Even though only one set of good quantitative measurements could be obtained so far, the two sets of velocity values clearly show that different nerve fibre groups have different temperature dependences of their group conduction velocity.

The SP2 afferents and the α_2 -motoneurons showed the same temperature dependence of the group conduction velocity. The calibration relation of the velocity distributions of afferent and efferent fibres, namely that the SP2 fibres conduct with the same velocity as the α_2 -motoneurons, is therefore temperature independent.

Nerve root cross-section and axon numbers

Table 1 of Ref.64 shows root diameter values. They vary between 0.31 and 1.6 mm, depending on the root level. Root S5 has a mean diameter of 0.47 mm and the dorsal root S4 has 0.62 mm. It cannot be excluded that in some cases dorsal root fascicles of more rostral roots were measured together with the S5 root. The diameters were calculated from the cross-sectional areas. Also, the percentual contributions of arteries and veins to

the cross-sectional area are listed in Table 1 of Ref. 64. As can be seen from Table 1 of Ref. 64, in thin roots the blood vessels can cover more than 50% of the cross-sectional area. For blood vessel diameters of nerve roots, further nerve root diameters and nerve root fibre counts see Refs. 35, 36, 62, 63.

Representative 350 to 500 fibres were measured in each root. The total number of nerve root fibres was obtained by comparing the area of the measured fibres with the area of all nerve root fibres in the root. The S4 ventral root was measured completely.

The numbers of myelinated fibres increased towards more rostral roots from 900 to 31,600. Root S5 contained on average 2900 fibres. Most myelinated fibres were found in the myelin sheath thickness class $0.25 \leq d < 0.8 \mu\text{m}$ followed by the class of thick myelin sheaths ($1.8 \leq d < 2.5 \mu\text{m}$). Few nerve fibres had a myelin sheath thickness between 0.8 and 1.8 μm .

The small number of nerve fibres in the S5 root suggests that this root is mostly not important for pelvic organ innervation. This is actually the reason why the S5 root (dorsal plus ventral) was normally cut in patients and obtainable for research. The unimportance for urinary bladder function was verified in the operation by not having a bladder pressure increase due to electrical stimulation of the S5 root. Sometimes a substantial urinary bladder pressure increase was obtained upon electrical stimulation of the S5 root. In such cases, the dorsal root was separated and removed and the ventral S5 root saved for electrical stimulation for bladder control.

Velocities of urinary bladder afferents

Urinary bladder afferent activities for constructing conduction velocity distribution histograms were recorded at bladder fillings of approx. 200 ml, depending on the compliances of the bladders measured preoperatively.

The thin bladder afferents with small AP amplitudes and long AP durations (M, S2; Fig. 11, Table 1 of Ref. 64) (possibly also activated by the bladder catheter) could not reliably be detected so far because of not good enough recording conditions.

Activity of urinary bladder afferents to retrograde bladder filling

For measuring bladder afferent activity increase upon retrograde bladder filling, the bladder was emptied and then filled while recording (time consuming procedure, successful so far only in two cases). With the groups of nerve fibres identified from conduction velocity distribution histograms, the increase in activity of the urinary bladder stretch (S1) and tension receptor afferents (ST) to retrograde bladder filling can be measured.

Fig. 7 shows the activity increases following filling of the bladder of para 7, via a catheter, with up to 400 ml fluid. The bladder was filled to the maxi-

mal acceptable value as determined pre-operatively by compliance (bladder filling volume / bladder pressure) measurements. Fig. 7B shows the sum of the individual velocity distributions for different filling stages for afferents and efferents. The peaks are identified by two calibration relations; α_2 -motoneurons conduct with the same velocity as the secondary muscle spindle afferents (~50 m/s); and α_3 -motoneurons conduct with the same group velocity as the stretch receptor afferents S1 (41 m/s) at about 35.5°C.

Fig. 7A gives velocity distributions for certain bladder filling stages. The most important obvious feature is that the bladder stretch and tension receptor afferents fire considerably even with no bladder filling.

By setting up conduction velocity borders of the S1 and ST groups according to the distribution curve (Fig. 11, inset), the activity of each group could be measured for different filling volumes and plotted (Fig. 8A). As can be seen in Fig. 8A, the stretch (S1) and tension receptor afferents (ST) in the left root S5 fired with 15 APs during 0.2 s at no bladder filling. The bladder afferents increased their firing with the increasing bladder storage volume. At 160 ml filling, a transient very strong firing of ST afferents occurred. This was the filling volume at which before the surgery the detrusor was activated in an urodynamic measurement. So far, it has not been possible to activate the detrusor with retrograde bladder filling during the surgery, even despite the light anesthesia (paraplegics with a complete spinal cord lesion feel no pain).

From a ventral S3 root in paraplegic 11, a similar undulating activity increase of S1 and ST bladder afferents was obtained with retrograde bladder filling. When the bladder was empty, the afferents (S1 and ST) fired already with 10 APs/0.2 s. At 50 ml filling, they fired with 23, at 200 ml with 6 at 250 ml with 25 and at 500 ml with 12 Aps/0.2 s. The detrusor was activated pre-operatively at a filling volume of 80 ml (continuously undulating contractions (0.08 Hz) started). As in the para 7, the first high afferent input falls approximately together with the onset of the pre-operative detrusor contraction, when filling the bladder. The occurrence of bladder afferent APs in the ventral S3 root was higher (166 APs/2.2 s) during the bladder filling than those of α -motoneuron APs (70 APs/2.2 s); the secondary muscle spindle afferents fired with 64 APs/2.2 s. The

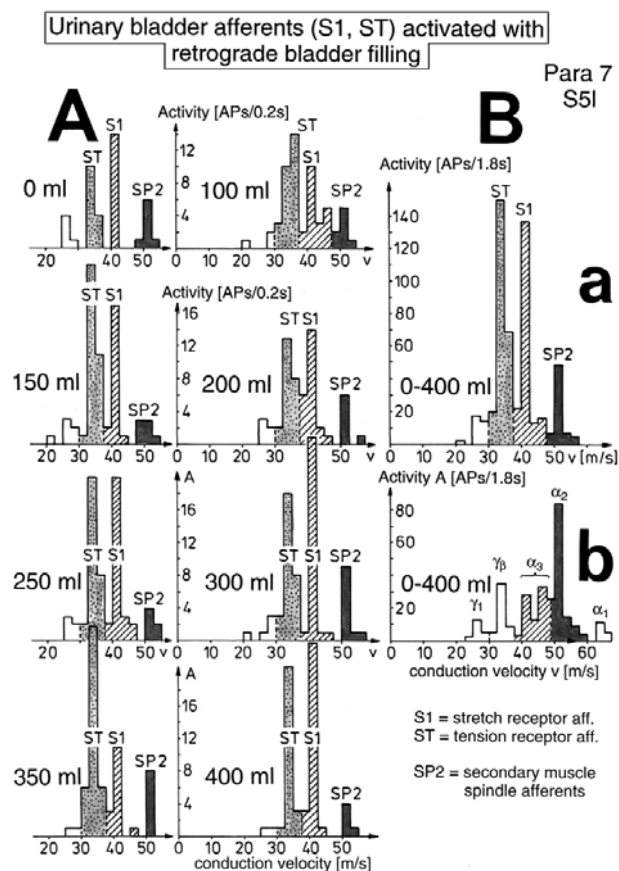


Fig. 7. – Conduction velocity distribution histograms for stretch (S1) and tension receptor afferents (ST) and secondary spindle afferents (SP2) for different retrograde filling stages of the urinary bladder (A). Summed histograms for afferents (a) and efferents (b) are plotted in B. α_1 , α_2 , γ_1 , γ_2 represent velocity distributions of α_1 , α_2 , γ_1 and γ_2 -motoneurons. Para 7, left nerve root S5.

speed of filling in para 11 was 300 ml/min. In this ventral S3 root there were at least a few percent of the fibres afferent.

Comparison of bladder afferent activity increase to bladder filling between a paraplegic and a brain-dead

The pathology of the bladder afferent activity in the paraplegic 7 analyzed in Fig. 8A, with dyssynergia of the bladder, is fully revealed by a direct comparison with the activity increase of the bladder afferents following retrograde bladder filling in brain-dead human HT6 (Fig. 8B). The dependence of the bladder afferent activity on the bladder filling volume in paraplegic 7 shows 4 main differences in comparison to those in HT6. (1) The bladder afferents already fired with no bladder filling which was not the case in HT6. (2) The activity increased more smoothly in HT than in the paraplegic, even though bladder filling was stopped 2 times in HT6 but was not stopped in para 7. (3) In the para 7 the tension receptor afferent activity was higher than the stretch receptor afferent activity which was not the case in HT6. (4) The bladder afferent activity was higher in the paraplegic than in the HT6. By taking into account the different measuring times of the activity, the ST-activity in para 7 was approx. 40 times higher than those in HT6 (210APs/1.2 s in para 7 against 5APs/1.2 in HT6). The recording conditions are not directly comparable. However, there are on average more bladder afferents in a root dS4 (HT6) than in a root S5. Still, the 40 times higher tension receptor afferent activity is probably overestimated. It is nevertheless safe to conclude that in some paraplegics the bladder afferent activity, especially from tension receptor afferents, was several times higher than that in the brain-dead human, the latter probably representing the physiologic case in this respect. The finding of an increased afferent activity in two paraplegics is in accordance with the experience that in brain-dead humans activity from bladder afferents was recorded only occasionally, whereas in paraplegics the activity from S1 and ST-afferents was always obvious and prominent in the velocity distributions, rather independent of the extent the bladder was filled. Paraplegics with dyssynergia of the bladder suffer from high bladder pressure. As will

Urinary bladder afferent activity in dependence on retrograde bladder filling

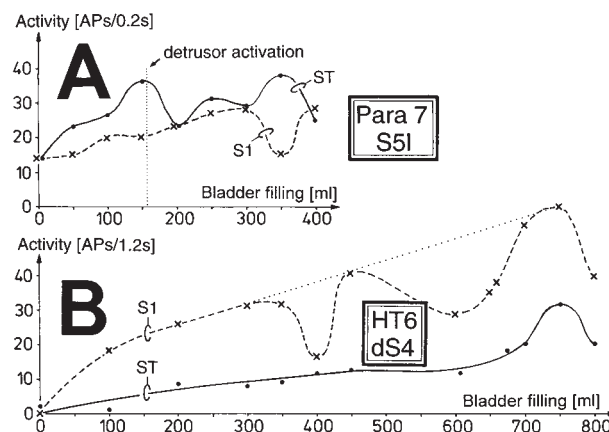


Fig. 8. – Afferent activity increase of stretch (S1) and tension receptor afferents (ST) to retrograde bladder filling in paraplegic 7 (left root S5) in relation to those of the brain-dead human HT6 (dorsal root S4). APs = action potentials. The speed of filling was 130 ml/min in para 7 and 100 ml/min in HT6.

be shown in the following papers (51, 52), this increased afferent activity will have consequences on the excitation of the CNS activating the striated sphincters of the bladder and the rectum.

Electrical intravesical stimulation

In Fig. 10A the recording and stimulation layout for electrical intravesical stimulation is shown. The negative electrode was connected to the tip of the bladder catheter, but was in no direct contact with the bladder mucosa. The indifferent positive electrode was attached to the leg of the patient. Following stimulation with 30V compound action potentials (CAPs) of stretch (S1) and tension receptor afferents (ST) could be evoked. In the recording from the root dS2 (Fig. 9A) mainly two CAPs follow the stimulation artefact, with latencies of 7.4 ms and 9.5 ms. The CAP conduction velocities in Fig. 9C were 41 and 35 m/s. According to Fig. 2B, the stretch receptor afferents contributed to the CAP with a latency of 7.4 ms and the tension receptor afferents to the CAP with a latency of 9.5 ms. The faster conducting S1 afferents give rise to the CAP with the shorter latency, as they would be expected to. From the latency and the group conduction velocity it can be calculated that the afferent activity traveled

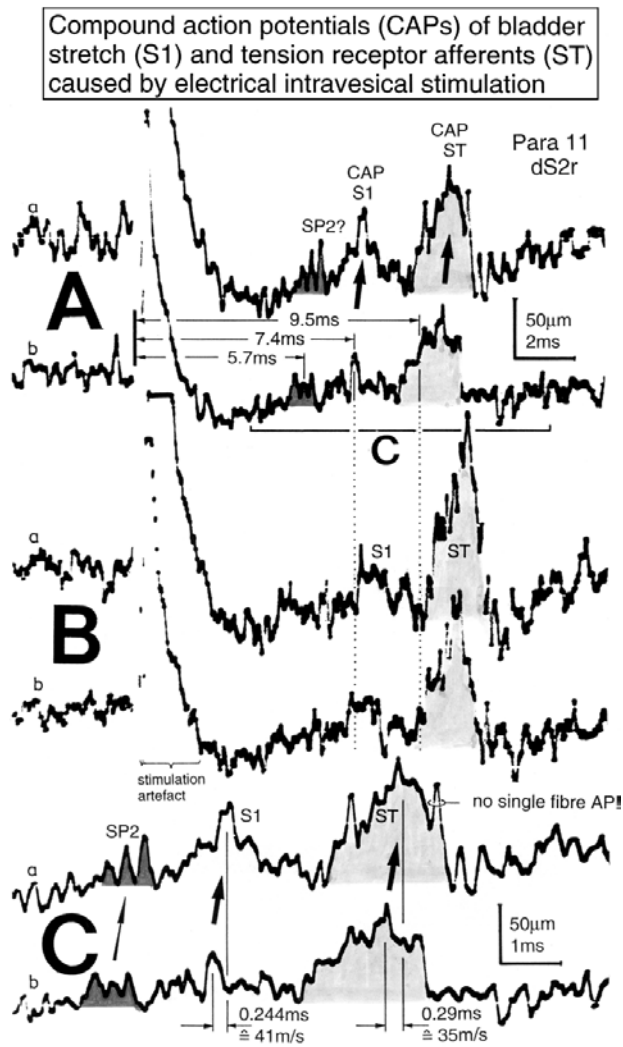


Fig. 9. – Compound action potentials (CAPs) of urinary bladder stretch (S1) and tension receptor afferents (ST) following electrical intravesical stimulation. Stimulation in B was slightly stronger than in A. The recordings in C represent a time-stretched portion of A. Mean conduction times and calculated mean conduction velocities of CAPs are indicated. In C, three single secondary muscle spindle afferent fibres are marked (SP2). The stimulation pulse (not rectangular) was 0.3 ms long; no earthing between recording and stimulating electrodes. Earth electrodes positioned 5 to 10 mm away from the recording electrodes reduced stimulation artefact and single fibre AP amplitudes and were therefore not used. Horizontal line of stimulation artefact is due to the limited input range.

approx. 320 mm to reach the recording electrodes, as indicated in Fig. 10A. The surgeon estimated a distance of 300 mm.

With a slightly increased electrical stimulation, the S1 and ST CAPs increased slightly (Fig. 9B),

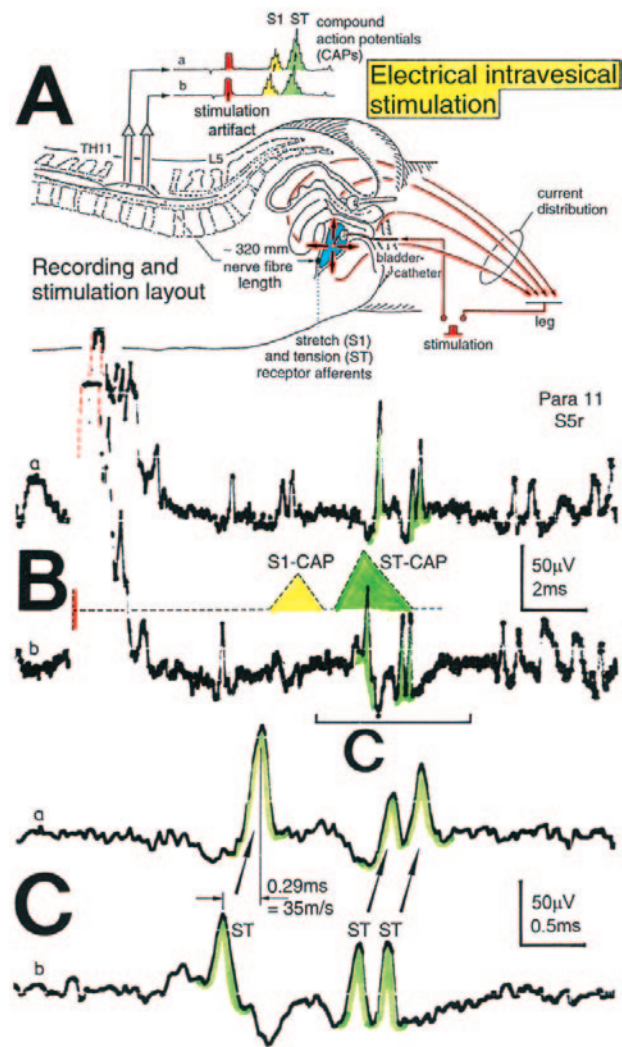


Fig. 10. – A. Recording and stimulation layout for electrical intravesical stimulation (electro negativity in bladder). B. Recording from an S5 root following electrical stimulation. Compound action potentials (CAPs) of S1 and ST afferents schematically redrawn from Fig. 9A. C. Time-stretched sweep piece of the recording in B. Single tension receptor afferent APs (ST) are indicated.

probably because more afferents were stimulated in the bladder wall. A recording from root S5 (same electrical stimulation) showed no pronounced CAPs. By schematically plotting S1 and ST CAPs from Fig. 9A into Fig. 10B and by calculating the conduction velocities of the single-fibre APs in the latency range of the ST CAP, it was found that the single-fibre APs were conducted by tension receptor afferents as can be seen from the time-stretched Fig. 10C. Thus at least the ST CAP was composed

of the single-fibre APs of the ST afferents. Normally, subpeaks in CAPs do not represent single-fibre APs as is indicated in Fig. 9C. The arithmetic addition of single-fibre APs of different triphasic AP wave forms often results in large amplitude potential changes, which do not represent single-fibre APs as can be learned from recordings of high skin afferent activity. To obtain CAP recordings from stretch and tension receptor afferents a substantial number of bladder afferents have to be stimulated simultaneously, through the nerve root which is used to record from.

Discussion

Unchanged conduction velocities and nerve fibre diameters

A classification scheme for the human peripheral nervous system has been developed by measuring conduction velocities and fibre diameters of single nerve fibres in brain-dead humans and patients with no spinal cord lesion, based on a new recording technique in man, the single-nerve fibre action potential (AP) recording from whole human sacral nerve roots, and a further developed morphometry allowing to group fibre diameters into 4 ranges of myelin sheath thickness (Fig. 1) (39, 45). Moreover, a new treatment has been developed (called coordination dynamics therapy), based on human neurophysiologic research of earlier, this, and the following papers, which can cure urinary bladder function (78, 86, 87) and can partially cure motor functions in humans with spinal cord injuries (67, 68, 84-87). Still the out-of-date bladder treatment, namely the electrical sacral anterior root stimulation, according to Brindley (7), is discussed here mainly for scientific reasons. The treatment involves deafferentation of the bladder to increase bladder storage volume, and electrical stimulation of the motoneuron and pre-ganglionic parasympathetic axons in the motor roots of the cauda equina. A precise electrodiagnosis during the surgery is crucial for the cutting of the bladder afferents and the saving of the motoneurons, and is performed by nerve root stimulation and bladder pressure measurements. The recording of single-fibre APs and compound APs brings about an improvement of the intraoperative diagnosis. A more selective cutting of afferents and partial saving of affer-

ents transmitting sexual sensations would improve the treatment. The hope is, that the dorsal S2 root contains many afferents conducting sexual sensitivity and only few conducting bladder fullness. The detailed representation of the urinary bladder and sexual organs in the sacral roots is still unclear. The representation varies among patients (4). Further, little is known which fibres conduct sexual feeling; the touch 4 (T4) (may be SAII) skin afferents ('Streichel receptor afferents') (44) probably contribute to it. A case is known, in which a lady with a partial spinal cord lesion was operated for urinary bladder control by electrical anterior root stimulation. The dorsal S2, S3 and S4 roots and the whole S5 root were cut. The sexual sensitivity was partly preserved. Some sexual organ afferents may therefore also run through the plexus hypogastricus or the dorsal S1 root. Ventral root afferents are probably too few to account for the preservation of sexual feeling. Morphometric analyses may help to clarify the nerve fibre group composition of nerves innervating pelvic organs (42), since the tapering of nerve fibres is very small (0.2% per 13 cm (70)). This new intraoperative electrodiagnosis may be of importance for refined surgical treatments.

The availability of single-fibre AP recordings and of dorsal roots, in which also dorsal root efferents are contained in the lower sacral nerve roots (39, 46), allowed me to simultaneously measure conduction velocities and fibre diameters of single afferent and efferent nerve fibres. Group conduction velocities and group nerve fibre diameters could be obtained from distribution histograms, similarly as in earlier measurements in brain-dead humans. The group conduction velocities and group nerve fibre diameters (peak values) obtained for paraplegics were found to be very similar to those estimated for brain-dead humans and patients with no spinal cord lesion. Thus, the classification scheme of the human peripheral nervous system is preserved at least 0.5 to 6 years following spinal cord lesion (Fig. 11). The subdivision of the α_1 -motoneurons (FF) in α_{11} , α_{12} and α_{13} -motoneurons needs further clarification.

The preservation of the classification scheme is not a trivial conclusion since changes occur in the peripheral and central nervous system following spinal cord lesion. It has been shown in this paper, that at least for some patients, the tension receptor afferents of the bladder fired even when the urinary

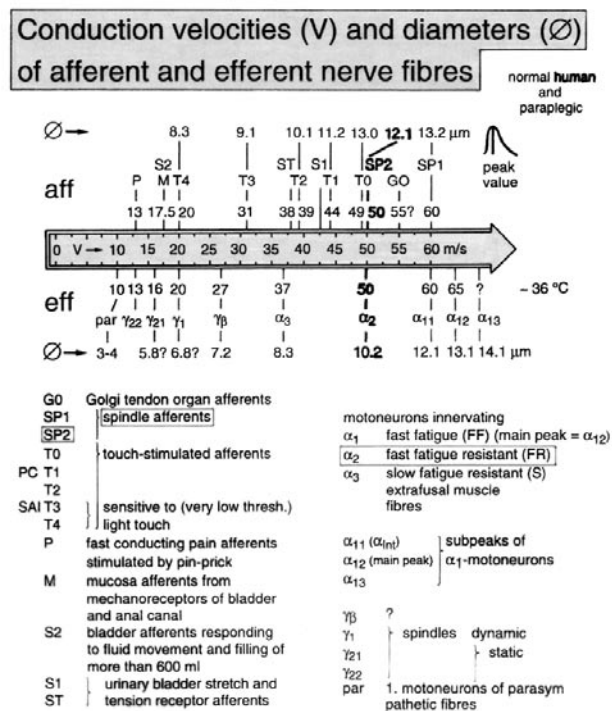


Fig. 11. – Conduction velocities (V) and nerve fibre diameters (\varnothing) of afferent and efferent nerve fibre groups in normal humans and in patients with a traumatic spinal cord lesion present for 0.5 to 6 years. The splitting of the α_1 -motoneurons into 3 subgroups, α_{11} , α_{12} , α_{13} , has not yet been confirmed.

bladder was empty. In the following papers (51, 52) it will be shown that functions of the spinal neuronal network change after injury, as judged by the impulse patterns of secondary muscle spindle afferents and spinal oscillators.

Classification schemes

The classification schemes of Grundfest, Erlanger and Gasser and Lloyd and Hunt (1, 3, 6, 11, 16, 20, 21, 27, 29-31) do not apply to humans and are too inaccurate to be used for detailed analyses of human nervous system functions. The differentiation between α_1 (FF), α_2 (FR) and α_3 (S)-motoneurons (9, 12, 18, 24, 39, 45) is essential for the understanding of CNS functions, since the three α -motoneuron types are integrated in functionally different spinal circuitries, and can be distinguished from each other by the different oscillation frequencies and impulse trains (high activity mode) (40, 52), different recruitment in the occasional firing mode (low activity mode)

(47, 48) and different motoneuron drive (52). The existence of slow and fast systems in the CNS has already been suggested by Sherrington (53).

There have been no other authors dealing seriously with the measurements of urinary bladder afferents in humans (39, 40). Animal data (13-15, 22) are unsuitable for a direct comparison with human data, unless the classification schemes for animals are improved, which has been started (9, 45, 47, 49). The differentiation between stretch and tension receptor afferents (39, 40) will contribute to the understanding of pathologic micturition.

It has been tried to applicate classification schemes to myenteric neurons (5, 59).

Temperature dependence of the conduction velocity

The conduction of APs in nerve fibres depends strongly on the temperature both in humans (Table 1 of 64, section 'temperature dependence of group conduction velocities') and animals (29). The increase of the conduction velocity of α_2 -motoneurons and secondary muscle spindle afferents results to approximately $2.8 \text{ m/s} / ^\circ\text{C}$. In humans, a temperature dependence of $2.1 \text{ m/s} / ^\circ\text{C}$ was measured; no differentiation between different groups was made (8). In animals, a temperature dependence of $3.5\% / ^\circ\text{C}$ was measured (30); data for different groups were not given. In this paper it was measured that in humans the temperature dependence of nerve fibre groups is different for the different groups. The effect of a strong temperature reduction is that the conduction velocity distribution peaks fuse, and it becomes difficult to identify the groups (peaks) (see Fig. 2 of (48)). In particular the preganglionic parasympathetic motoneurons can be better differentiated from the static γ -motoneurons at a root temperature higher than 35°C . The temperature of the thin roots is not exactly measurable. Efforts should be spent to keep the temperature in the operational field close to the central temperature of the patient. In the future, conduction velocities obtained from the roots of the cauda equina have to be calibrated using conduction velocities obtained non-invasively from the same fibres of the leg. Such a comparison requires an analysis of CAPs with single-fibre APs (50).

Identification of nerve fibre groups however does not depend on the knowledge of the exact conduc-

tion velocity: conduction velocity distribution histograms can be calibrated using the same velocity of conduction by α_2 -motoneurons and secondary muscle spindle afferents (SP2), α_3 -motoneurons and stretch receptor afferents of the bladder (S1), and approximately by α_1 -motoneurons and primary spindle afferents (SP1). The SP2 fibres and the α_2 -motoneurons showed the same temperature dependence of the conduction velocity; this calibration relation is therefore temperature independent in the temperature range 32 to 36°C.

Recording of APs from preganglionic parasympathetic motoneurons

In a first approximation the AP amplitude depends on the diameter of the axon, and declines due to volume conductance if the axons are not positioned close to the recording electrodes (see Method). Thinner axons have smaller AP amplitudes than thicker ones (37), even though the area between the AP curve and the baseline is, in a first approximation independent of the AP amplitude (50), because the AP duration increases for thinner, slower conducting fibres (30, 31, 37). The preganglionic parasympathetic motoneurons with a peak group diameter of approx. 3.5 μm have very small AP amplitudes (and very long duration) (Fig. 3D), so that they are difficult to recognize in the noise and artefact level, and are often overshadowed by large APs of thick fibres. Even though most likely, parasympathetic action can also be estimated from the impulse patterns of secondary muscle spindle afferents (49, 51), sometimes it is very important to obtain impulse patterns of single preganglionic parasympathetic motoneurons. Only in this way it is possible to analyze neuronal networks of the sacral micturition center. The asymmetrical distribution of preganglionic parasympathetic axons with a nerve fibre diameter of up to 6 μm will sometime make it possible to safely record parasympathetic APs and to extract natural impulse patterns of single fibres from the recordings, provided good recording conditions. Thin ventral S4 roots freed over long sections from other roots, with nearly no shunting blood vessels (see Method), are favorable for recording single-fibre APs in patients with no arachnoiditis.

Extension of the classification scheme to thinner fibres

As discussed above for the preganglionic parasympathetic motoneurons, the limit for recording single-fibre APs from undissected roots or fascicles are diameters between 3 and 4 μm . It was recorded therefore from myelinated fibres only. This does not mean that it is impossible to record from unmyelinated fibres. It should be possible to record extracellular APs from unmyelinated human axons thicker than 4 μm .

To extend the classification scheme of the human peripheral nervous system to nerve fibres thinner than 3 to 4 μm , CAPs have to be analyzed with the single-fibre AP recording method to identify the nerve fibre group composition, as has been begun (50). This seems possible since the radial decline of the AP amplitude due to volume conductance (17) is reasonably small for very thin roots or fascicles. The area between the AP curve and the baseline is in a first approximation, the same for all nerve fibres, so that CAPs can be analysed with the simultaneously recorded single-fibre APs (50). In this way it seems possible to measure the conduction velocities of thin nerve fibre groups, in which the single-fibre APs cannot be recorded any more, using conduction velocities of CAPs (see Fig. 9C).

The identification of further peak group nerve fibre diameters is more difficult. Firstly, there are afferent nerve fibre groups with strongly overlapping diameter distributions, and afferent fibres cannot be distinguished from efferent fibres. For a further identification of nerve fibre group diameters peripheral nerves of known group composition have to be analyzed morphometrically; this work has already been started (41-44). A comparison of nerve fibre diameters of fibres of the spinal canal with those at more distance from the medulla in the periphery is possible (if there is no branching of fibres) because the tapering of nerve fibres is small (0.2% per 13 cm (70)).

Recording conditions

The optimal inter-electrode distance for obtaining the highest AP amplitudes is approximately 6 mm; the distance of 4 mm used was close to that value. Low-resistance electrical shunts reduce the AP

amplitude and result from the saline solution around the root filaments, the cerebral fluid (plus 0.9% NaCl from washing the roots) of the spinal canal connected via the root filaments emerging from the fluid, and the blood vessels in the root. The first low-resistance shunt is reduced by removing the saline film around the root (soaking up with a wet tissue and drying the root). The second shunt is reduced by lifting the up to 200 mm long root (35) 10 to 20 mm out of the cerebral fluid, which is not always possible (anatomical variation, arachnoiditis). Since thicker sacral nerve roots have comparably less contributions from blood vessels to the root cross-section than the thinner ones (Fig. 6A, Table 1 of 64), single-fibre extracellular APs can be recorded up to a fascicle diameter of 1 mm. S4 ventral roots are ideal for recording, because they are thin (large AP amplitude), contain not too many afferents (~1%, low activity) and somatic and parasympathetic afferents and efferents are contained. Drying up of roots should be avoided because of axonal damage; normally, drying up results in a dramatic activity increase of mirror-picture potentials (an AP generated between the electrode pairs travels ortho- and antidromically and shows an afferent wave form on one electrode pair trace (upwards) and an efferent form (downwards) on the other trace), and in seemingly very fast AP conduction. Wetting of the roots with 0.9% NaCl stops the generation of artifact potentials. Incorrect plugging of the wire electrodes can change the AP wave form. With the recording of touch activity (39, 44) it can easily be proved that the wiring is correct. One advantage of the recording with wire electrode pairs and differential input is that no Faraday cage (normally not available in operating theatres) is needed, which is an important point in this new recording technique. The unscreened length of the recording electrodes was about 15 mm. Further screening was achieved by positioning the platinum wires close to the electrode holder, made of bronze. Covering the operational area with mull soaked with 0.9% NaCl at 37°C creates a Faraday cage and a moist chamber (no drying up) and the temperature is kept more constant because of reduced evaporation. The exact measurement of the root temperature is a problem; in the future it might partially be solved by comparing conduction velocities measured from nerve roots of the opened spinal canal, with those of the lower limbs where the tem-

perature can easily be measured. For such comparisons conduction velocities of nerve fibre groups in limb nerves have to be defined according to the classification scheme of the human peripheral nervous system and measured exactly. Paraffin oil cannot be used during the surgery. Also, paraffin oil changes the excitability of membranes (19).

Unchanged axon numbers and axon densities of the lower sacral nerve roots following spinal cord lesion

Fig. 6A shows different nerve root cross-sections. It can be seen that the right root dS4 is approximately twice as thick as either root vS4 or root S5. Root dS2 is approximately 4 times (2×2) as thick as root dS4. The findings are in accordance with the measurements on human cadavers, showing that dorsal roots in the sacral segments are approx. twice as thick as the ventral ones, and that ventral or dorsal sacral roots (~5 cm away from the medulla) are of approx. twice the diameter of the adjacent caudal root (36).

The dorsal S2 root (Fig. 6A) has approx. 31,600 myelinated axons (patient aged 25 years). Humans aged 47-85 years without spinal cord lesions had 28,000 myelinated axons in the dorsal S2 root. Since the number of axons (and the nerve conduction velocity) reduces with the age (28), it can be stated that the fibre number in the dorsal S2 root did not change following spinal cord lesion. The axon density in the S2 root is $a = \text{number}/d^2\pi/4 = 31600/2 = 15,800$ myelinated axons / mm². For normal humans (age 47-85 years) the axon density per mm² is 12,000 (36). Allowing for age, these values are very similar again. The three roots dS4 shown in Table 1 had mean myelinated axon numbers of 6600 and a mean density of 22,600 axons per mm² (age 26 years). Comparable values for normal (older) humans are 4800 axons and 13,800 axons / mm² respectively. With age taken into account, it can be concluded that the number of fibres in the sacral dorsal roots had not changed following spinal cord lesion. The ventral S4 root in Fig. 6A contained 900 myelinated fibres and had a myelinated axon density of 12,000 per mm². The values for the normal (older) population are 800 myelinated axons and 9,000 myelinated axons / mm² [36]. Again, the values for the ventral root in the paraplegics are very

similar to those for the normal population. Even though the evidence has been based on a few cases, it can be concluded that the numbers of myelinated fibres in dorsal and ventral lower sacral nerve roots did not change 0.5 to 6 years following a spinal cord lesion.

Further, hemorrhagic necrosis and oedema affect the cord segments adjacent to the injured cord segment. Later changes include gliosis along the degenerating tracts which normally connect the sacral cord and brain. Some patients with complete lesions well above the level of the sacral cord also have evidence of trauma or infarction of the lumbosacral cord. Such patients have a flaccid bladder, and little sphincter tone. These pathological changes may partly explain the variation that can be seen in urodynamic findings of groups of paraplegic patients in some studies (54, 56). Since the number of myelinated fibres in the sacral nerve roots did not change (no evidence of motoneuron cell death), and the operated paraplegics had a spastic bladder, it is unlikely that the necrosis reached the sacral spinal cord. Because interneuron cell death has also not been found so far, bladder dysfunction probably results from changed afferent input to the spinal cord and a disorganization of the neuronal networks of the isolated cord (see below).

Increased bladder afferent activity as one origin reason for urinary bladder dysfunction

It has been shown above, by comparing with normal values, that the numbers of myelinated fibres and the density of myelinated nerve fibres in the lower sacral ventral and dorsal roots did not change following spinal cord lesion. Also, it has been shown, based on a comparison with values for brain-dead humans and patients with no spinal cord lesion, that the values of group conduction velocities and group nerve fibre diameters remained unchanged. Thus, the nerve fibres of the peripheral nervous system were not affected by any change following spinal cord lesion unless some additional degenerative process had occurred in the periphery (nerve roots emerging from the medulla close to the spinal cord lesion will have changed nerve fibre numbers because of a damage also to the gray matter). This does not mean however that the impulse traffic has not

changed. A dramatic increase in the activity of the stretch (S1) and tension receptor afferents (ST) was shown with certainty in two paraplegics (Fig. 8). Also, in several other patients' bladder afferent activity seemed increased, as the bladder afferent activity was prominent for even small bladder filling volumes. Nearly all patients who underwent surgery had a much smaller storage volume of the urinary bladder, but not necessarily a reduced compliance (filling volume / pressure ratio). Following urinary bladder deafferentiation the bladder storage volume increased as did the compliance. However, there are also paraplegics with a storage volume of 50 ml and no increased compliance. They are said to have hyperreflexia of the bladder. Thus, there are patients with a stiff and infected bladder in whom the afferent activity of the bladder is much higher (see also (51)). The afferent activity is often even present with an empty bladder. The increased bladder afferent activity causes the detrusor being activated too early (52). On the other hand, there are patients with no increased compliance and no infection, and a detrusor which already contracts at filling volumes of 50 ml. It will be shown in the two following papers (51, 52) that there are important changes in the somatic and parasympathetic neuronal network of the sacral micturition center and in the coordination between them; this can account for a too early activation of the detrusor and the external sphincter. It will further be shown in a following paper (78) that most of the complications of urinary bladder functions can be avoided and urinary bladder functions be cured if the learning-based movement therapy, called 'coordination dynamics therapy', is started early after the spinal cord injury (best 1 or 2 weeks after injury) and is administered for 3 years.

Electrical intravesical stimulation and clinical implications

Electrical stimulation of the nearly empty urinary bladder with 30 V (0.3 ms pulse duration, negative electrode in the bladder, contact gel used) evoked CAPs of bladder stretch and tension receptor afferents. Even though more experience is needed to reliably activate the bladder afferents by electrical stimulation, the group conduction velocities of bladder afferents obtained from the CAPs were in accor-

dance with the values obtained from single-fibre AP recordings. This accordance is of importance at least for two reasons. Firstly, there are no other precise data on human urinary bladder afferents available. The support by another method gives more safety. Secondly, if intravesical stimulation can be used as a reliable identification tool of urinary bladder afferents, the diagnosis of bladder innervation during a surgery can be more refined and provide for a more selective deafferentation and more selective electrical stimulation, thus improving this method of (invasive, destructive, non-causal) treatment. Also, the possible biological approach of improving urinary bladder function by a nerve anastomosis from the lower intercostal nerves to the cauda equina nerve roots with respect to functional aspects (invasive, partly destructive, only partly causal) (41-44) needs extremely detailed knowledge of the bladder innervation and function, and intraoperative verification of afferent and efferent fibres innervating the bladder, as the representation of the urinary bladder in roots S2 to S5 (mainly S3 and S4) varies.

Proper treatment of urinary bladder function

Since coordination dynamics therapy can improve CNS motor functions in incomplete spinal cord injury (67) till to a near-total cure (68, 86) and can cure urinary bladder function in severe cervical spinal cord injury (78), the sacral anterior root stimulation according to Brindley (7) and the intercostal nerve to cauda equine nerve root anastomosis to improve urinary bladder functions (41-44) are not justified any more in (young) patients with spinal cord injury, because they are destructive treatments. Coordination dynamics therapy on the other hand is a causal natural learning-based movement therapy, in which the patient is not losing any function. He can only regain further functions. Why administering destructive non-causal treatments if a better causal one is available? At the beginning of this research project, I developed myself a nerve anastomosis operation for urinary bladder control (most important function for patients to be reconstructed) on a high scientific level (41-44), but I did not want to apply the treatment at the end because it was still a destructive operation. Patients with spinal cord injury (especially in severe cervical spinal cord injury)

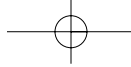
have so little functions left that they should not lose any further functions with the treatment. For scientific reasons however it is still interesting to discuss these treatments. Also, there may be patients who do not want to train or cannot perform a movement therapy for other reasons. For them there would then be still these treatments available.

References

1. ARBUTHNOTT, E.R., BOYD, I.A. and KALU, K.U.: Ultrastructural dimensions of myelinated peripheral nerve fibre in the cat and their relation to conduction velocity. *J. Physiol.*, 308: 125-157, 1980.
2. BEHSE, F. and BUCHTHAL, F.: Normal sensory conduction in the nerves of leg in man. *J. Neurol. Neurosurg. Psychiat.*, 34: 404-414, 1971.
3. BOYD, I.A. and DAVEY, M.R.: Composition of peripheral nerves. Livingston, Edinburgh, 1968.
4. BOHM, E.: Sacral rhizopathies and sacral root syndroms (SII-SV). *Acta Chir. Scand.*, 216: 5-48, 1956.
5. BORNSTEIN, J.C., FURNESS, J.B. and KUNZE, W.A.A.: Electrophysiological characterization of myenteric neurons – How do classification schemes relate (Review). *J. Auton. Nerv. Syst.*, 48: 1-15, 1994.
6. BOYD, I.A. and KALU, K.U.: Scaling factor relating conduction velocity and diameter for myelinated afferent nerve fibres in cat hindlimb. *J. Physiol.*, 289: 277-297, 1979.
7. BRINDLEY, G.S., POLKEY, C.E., RUSHTON, D.N. and CARDOZZO, L.: Sacral anterior root stimulation for bladder control in paraplegia: the first 50 cases. *J. Neurol. Neurosurg. Psychiat.*, 49: 1104-1114, 1986.
8. BUCHTHAL, F. and ROSENFALCK, A.: Evoked potentials and conduction velocity in human sensory nerves. *Brain Research*, 3: 1-122, 1966.
9. BURKE, R.E., LEVINE, D.N., TSAIRIS, P. and ZAJAK III, F.E.: Physiological types and histochemical profiles in motor units of the cat gastrocnemius. *J. Physiol.*, 234: 723-748, 1973.
10. DORFMAN, L.J., CUMMINS, K.J. and LEIFER, L.J.: Conduction Velocity Distributions – A Population Approach to Electrophysiology of Nerve, Alan R. Liss, Inc., New York, 1981.
11. ERLANGER, J. and GASSER, H.S.: Electrical signs of nervous activity. Philadelphia, University of Pennsylvania Press, 1937.
12. FLESHMAN, J.W., MUNSON, J.B., SYPERT, G.W. and FRIEDMAN, W.A.: Rheobase, input resistance, and motor unit type in medial gastrocnemius motoneurons in the cat. *J. Neurophysiol.*, 41: 1326-1338, 1981.
13. GARRY, R.C. and GARVEN, H.S.D.: The ganglia, afferent endings and musculature of the urethra in the cat. *J. Physiol.*, 139: 1P-2P, 1957.
14. GARRY, R.C., ROBERTS, T.D.M. and TODD, J.K.: Reflex responses of the external urethral sphincter of the cat to filling of the bladder. *J. Physiol.*, 139: 13P-14P, 1957.

15. GARRY, R.C., ROBERTS, T.D.M. and TODD, J.K.: Reflexes involving the external urethral sphincter in the cat. *J. Physiol.*, 149: 653-665, 1959.
16. GASSER, H.S. and GRUNDFEST, H.: Axon diameter in relation to the spike dimension and the conduction velocity in mammalian A fibres. *Am. J. Physiol.*, 127: 393-414, 1939.
17. GATH, I. and STAHLBERG, E.: On the volume conduction in human skeletal muscle: in situ measurements. *Electroencephalo. Clin. Neurophysiol.*, 43: 106-110, 1977.
18. GUSTAFSON, B. and PINTER, M.J.: Relations among passive properties of lumbar α -motoneurons of the cat. *J. Physiol.*, 356: 401-431, 1984.
19. HODGKIN, A.L.: The local electric changes associated with repetitive action in a non-medullated axon. *J. Physiol.*, 107: 165-181, 1948.
20. HUNT, C.C.: Relation of function to diameter in afferent fibres of muscle nerve, *J. Gen. Physiol.*, 38: 117-131, 1954.
21. HURSH, J.B.: Conduction velocity and diameter of nerve fibres. *Am. J. Physiol.*, 127: 131-139, 1939.
22. IGGO, A.: Tension receptors in the stomach and the urinary bladder. *J. Physiol.*, 128: 593-607, 1955.
23. JULIAN, F.J. and GOLDMANN, D.E.: The effect of mechanical stimulation on some electrical properties of axons. *J. Gen. Physiol.*, 46: 297-313, 1962.
24. KERNELL, D. and ZWAGSTRA, B.: Input resistance, axon conduction velocity and cell size among hindlimb motoneurons of the cat. *Brain Research*, 204: 311-326, 1981.
25. KOLLER, S., REICHERTZ, P.L. and ÜBERLA, K.: Medizinische Informatik and Statistik. Springer Verlag, Berlin, 1984.
26. KUGELBERG, E.: 'Injury activity' and 'trigger zones' in human nerves. *Brain*, 69: 310-324, 1946.
27. LLOYD, D.P.C.: Neuron patterns controlling transmission of ipsilateral hind limb reflexes in cat. *J. Neurophysiol.*, 6: 293-315, 1943.
28. LUDIN, H.P.: *Praktische Elektromyographie*, Enke Verlag, Stuttgart, 1993.
29. PAINTAL, A.S.: Effect of temperature on conduction in single vagal and saphenus myelinated nerve fibres of the cat. *J. Physiol.*, 180: 20-49, 1965.
30. PAINTAL, A.S.: The influence of diameter of medullated nerve fibres of cats on the rising and falling phase of the spike and its recovery. *J. Physiol.*, 184: 791-811, 1966.
31. PAINTAL, A.S.: Conduction in mammalian nerve fibres. In: J.E. Desmedt (Ed.). *New Developments in Electromyography and Clinical Neurophysiology*, Vol. 2, Karger, Basel, pp. 19-41, 1973.
32. ROSENFALCK, P.: Intra- and extracellular potential fields of active nerve and muscle fibres. A physio-mathematical analysis of different model. *Acta Physiol. Scand., Suppl.*, 321: 1-168, 1969.
33. RUDGE, P., OCHOA, J. and GILIATT, R.W.: Acute peripheral nerve compression in the baboon, *J. Neurological Sciences*, 23: 403-420, 1974.
34. RUSHTON, W.A.H.: Resistance artifact in action potential measurements. *J. Physiol.*, 104: 19P-20P, 1945.
35. SCHALOW, G.: The problem of cauda equina nerve root identification. *Zbl. Neurochir.*, 46: 322-330, 1985.
36. SCHALOW, G., AHO, A. and LANG, G.: Nerve fibre counts for an intercostal nerve to cauda equina nerve root anastomosis. *Zent. Bl. Chir.*, 112: 457-461, 1987.
37. SCHALOW, G. and LANG, G.: Electrodiagnosis of human dorsal sacral nerve roots by recording afferent and efferent extracellular action potentials. *Neurosurg. Rev.*, 12: 223-232, 1989.
38. SCHALOW, G.: Efferent and afferent fibres in human sacral nerve roots: basic research and clinical implications. *Electromyogr. Clin. Neurophysiol.*, 29: 33-53, 1989.
39. SCHALOW, G.: Conduction velocities and nerve fibre diameters of touch, pain, urinary bladder and anal canal afferents and α and γ -motoneurons in human dorsal sacral nerve roots. *Electromyogr. Clin. Neurophysiol.*, 31: 265-296, 1991.
40. SCHALOW, G.: Oscillatory firing of single human sphincteric α_2 and α_3 -motoneurons reflexly activated for the continence of urinary bladder and rectum. Restoration of bladder function in paraplegia. *Electromyogr. Clin. Neurophysiol.*, 31: 323-355, 1991.
41. SCHALOW, G., AHO, A. and LANG, G.: Microanatomy and number of nerve fibres of the lower intercostal nerves with respect to a nerve anastomosis. Donor nerve analysis. I (IV). *Electromyogr. Clin. Neurophysiol.*, 32: 171-185, 1992.
42. SCHALOW, G.: Number of fibres and fibre diameter distributions of nerves innervating the urinary bladder in humans. Acceptor nerve analysis. II (IV). *Electromyogr. Clin. Neurophysiol.*, 32: 187-196, 1992.
43. SCHALOW, G. and Barth, H.: Single-fibre action potential recording from the nerve to the musculus obliquus externus abdominis following pin-prick in humans. III (IV). *Electromyogr. Clin. Neurophysiol.*, 32: 197-205, 1992.
44. SCHALOW, G.: Impulse pattern, innervation density and two point discrimination of skin and mucosal afferents in humans. Consideration for a sensory reinnervation of urinary bladder and anal canal in spinal cord lesion. IV (IV). *Electromyogr. Clin. Neurophysiol.*, 32: 259-285, 1992.
45. SCHALOW, G. and BARTH, H.: Group conduction velocities and nerve fibre diameters of α and γ -motoneurons from lower sacral nerve roots of the dog and humans. *Gen. Physiol. Biophys.*, 11: 85-99, 1992.
46. SCHALOW, G.: Ventral root afferent and dorsal root efferent fibres in dog and human lower sacral nerve roots. *Gen. Physiol. Biophys.*, 11: 123-131, 1992.
47. SCHALOW, G. and WATTIG, B.: Recruitment of α and γ -motoneurons in rats, dogs and humans. *Electromyogr. Clin. Neurophysiol.*, 33: 387-400, 1993.
48. SCHALOW, G.: Recruitment of motoneurons in the occasional firing mode in paraplegics. *Electromyogr. Clin. Neurophysiol.*, 33: 401-408, 1993.
49. SCHALOW, G.: Action potential patterns of intrafusal γ and parasympathetic motoneurons, secondary muscle spindle afferents and an oscillatory firing α_2 -motoneuron, and the phase relations among them in humans. *Electromyogr. Clin. Neurophysiol.*, 33: 477-503, 1993.
50. SCHALOW, G. and ZÄCH, G.A.: Nerve compound action potentials analyzed with the simultaneously measured single-fibre action potentials in humans. *Electromyogr. Clin. Neurophysiol.*, 34: 451-465, 1994.

51. SCHALOW, G., BERSCH, U., GÖCKING, K. and Zäch, G.A.: Detrusor-sphincteric dyssynergia in paraplegics compared with the synergy in a brain-dead human by using the single-fibre action potential recording method. *J. Auton. Nerv. Syst.*, 52: 151-180, 1995.
52. SCHALOW, G., BERSCH, U. MICHEL, D. and KOCH, H.G.: Detrusor-sphincteric dyssynergia in humans may be caused by a loss of stable phase relations between and within oscillatory firing neuronal networks of the sacral micturition center. *J. Auton. Nerv. Syst.*, 52: 181-202, 1995.
53. SHERRINGTON, C.S.: Nervous rhythm arising from rivalry of antagonistic reflexes: Reflex stepping as outcome of double reciprocal innervation. *Proc. R. Soc. Lond. (Biol.)*, 86: 233-261, 1913.
54. THOMAS, D.G.: The urinary tract following spinal cord injury. In G.D. Chisholm and D.I. Williams (Eds.), *Scientific foundation of urology*, 2nd edn. Heinemann, London, pp. 421-433, 1982.
55. TOREBJÖRK, H.E., HALLIN, R.G., HONGELL, A. and HAGBARTH, K.-E.: Single unit potentials with complex wave form seen in microelectrode recordings from the human median nerve. *Brain Research*, 24: 443-450, 1970.
56. TORRENS, M. and MORRISON, J.F.B.: *The Physiology of the Lower Urinary Tract*, Springer Verlag, Berlin, p. 224, 1987.
57. VALLBO, A.B., HAGBARTH, K.-E., TOREBJÖRK, H.E. and WALLIN, B.G.: Somatosensory, proprioceptive, and sympathetic activity in human peripheral nerves. *Physiological Reviews*, 59: 919-957, 1979.
58. VALLBO, A.B.: Prediction of propagation block on the basis of impulse shape in single unit recordings from human nerves. *Acta Physiol. Scand.*, 97: 66-74, 1976.
59. WOOD, J.D.: Application of classification schemes to the enteric nervous system (Review), *J. Auton. Nerv. Syst.*, 48: 17-29, 1994.
60. WOODBURY, J.W.: Direct membrane resting and action potentials from single myelinated nerve fibres. *J. Cellular and Comparative Physiol.*, 39: 323-339, 1952.
61. ZOTTERMAN, Y.: Touch, pain and tickling: An electrophysiological investigation on cutaneous sensory nerves. *J. Physiol.*, 95: 1-28, 1939.
62. SCHALOW, G., AHO, A. and LANG, G.: Nerve fibre counts for an intercostal nerve to cauda equina nerve root anastomosis. *Zent.bl. Chir.*, 112: 457-461, 1987.
63. SCHALOW, G.: Feeder arteries, longitudinal arterial trunks and arterial anastomoses of the lower human spinal cord. *Zbl. Neurochir.*, 51: 181-184, 1990.
64. SCHALOW, G., ZÄCH, G.A. and WARZOCK, R.: Classification of human peripheral nerve fibre groups by conduction velocity and nerve fibre diameter is preserved following spinal cord lesion. *J. Auton. Nerv. Syst.*, 52: 125-150, 1995.
65. SCHALOW, G.: Stroke recovery induced by coordination dynamic therapy and quantified by the coordination dynamic recording method. *Electromyogr. Clin. Neurophysiol.*, 42: 85-104, 2002.
66. SCHALOW, G.: Improvement after traumatic brain injury achieved by coordination dynamic therapy. *Electromyogr. Clin. Neurophysiol.*, 42: 195-203, 2002.
67. SCHALOW, G.: Recovery from spinal cord injury achieved by 3 months of coordination dynamic therapy. *Electromyogr. Clin. Neurophysiol.*, 42: 367-376, 2002.
68. SCHALOW, G.: Partial cure of spinal cord injury achieved by 6 to 13 months of coordination dynamic therapy. *Electromyogr. Clin. Neurophysiol.*, 43: 281-292, 2003.
69. SCHALOW, G., PÄÄSUKKE, M., ERELIN, J. and GAPEYEVA, H.: Improvement in Parkinson's disease patients achieved by coordination dynamics therapy. *Electromyogr. Clin. Neurophysiol.*, 44: 67-73, 2004.
70. SCHALOW, G.: Tapering of human nerve fibres. *Gen. Physiol. Biophys.*, 24: 427-448, 2005.
71. SCHALOW, G., PÄÄSUKKE, M., JAIGMA, P.: Integrative reorganization mechanism for reducing tremor in Parkinson's disease patients. *Electromyogr. Clin. Neurophysiol.*, 45: 407-415, 2005.
72. SCHALOW, G., JAIGMA, P.: Cerebral palsy improvement achieved by coordination dynamics therapy. *Electromyogr. Clin. Neurophysiol.*, 45: 433-445, 2005.
73. SCHALOW, G.: Hypoxic brain injury improvement induced by coordination dynamics therapy in comparison to CNS development. *Electromyogr. Clin. Neurophysiol.*, 46: 171-183, 2006.
74. SCHALOW, G. and JAIGMA, P.: Improvement in severe traumatic brain injury induced by coordination dynamics therapy in comparison to physiologic CNS development. *Electromyogr. Clin. Neurophysiol.*, 46: 195-209, 2006.
75. SCHALOW, G.: Symmetry diagnosis and treatment in coordination dynamics therapy. *Electromyogr. Clin. Neurophysiol.*, 46: 421-431, 2006.
76. SCHALOW, G.: Cerebellar injury improvement achieved by coordination dynamics therapy. *Electromyogr. Clin. Neurophysiol.*, 46: 433-439, 2006.
78. SCHALOW, G.: Cure of urinary bladder function achieved in a patient with severe cervical spinal cord injury (95% injury) after 3 years of coordination dynamics therapy. *Electromyogr. Clin. Neurophysiol.*, submitted.
79. MARTINO, G. and PLUCHINO, S.: The therapeutic potential of neural stem cells. *Nat. Rev. Neurosci.*, 7: 395-406, 2006.
80. THURET, S., MOON, L.D.F. and GAGE, F.H.: Therapeutic interventions after spinal cord injury. *Nat. Rev. Neurosci.*, 7: 628-643, 2006.
81. BRADBURY, E.J. and MCMAHON, S.B.: Spinal cord repair strategies: why do they work? *Nat. Rev. Neurosci.*, 7: 644-653, 2006.
82. HAREL, N.Y. and STRITTMATTER, S.M.: Can regenerating axons recapitulate developmental guidance during recovery from spinal cord injury. *Nat. Rev. Neurosci.*, 7: 603-616, 2006.
83. KELSO J.A.S.: *Dynamic Patterns. The Self-Organization of Brain and Behavior*. MIT Press, Cambridge, 1995.
84. SCHALOW, G., VAHER, I. and JAIGMA, P.: Overreaching in coordination dynamics therapy in an athlete with a spinal cord injury. *Electromyogr. Clin. Neurophysiol.*, 48: 83-95, 2008.
85. SCHALOW, G.: Stem cell therapy and Coordination dynamics therapy to improve Spinal cord injury. *Electromyogr. Clin. Neurophysiol.*, in press, 2008.



86. SCHALOW, G., JAIGMA, P. and BELLE, V.K.: Near-total functional recovery achieved in partial spinal cord injury (50% injury) after 3 years of coordination dynamics therapy. Electromyogr. *Clin. Neurophysiol.*, in press, 2008.
87. SCHALOW, G.: Partial cure achieved in a patient with near-complete cervical spinal cord injury (95% injury) after 3 years of coordination dynamics therapy. Electromyogr. *Clin. Neurophysiol.*, submitted, 2008.

Address reprint requests to:
Giselher Schalow
Dr.med.habil., Dr.rer.nat., Dipl.Ing.
Untere Kirchmatte 6
CH-6207 Nottwil
Switzerland
www.cdt.host.sk
g_schalow@hotmail.com

